JCI The Journal of Clinical Investigation

RECON syndrome is a genome instability disorder caused by mutations in the DNA helicase RECQL1

Bassam Abu-Libdeh, … , Robert M. Brosh Jr., Grant S. Stewart

J Clin Invest. 2022. https://doi.org/10.1172/JCI147301.

Research In-Press Preview **Cell biology** **Genetics**

Graphical abstract

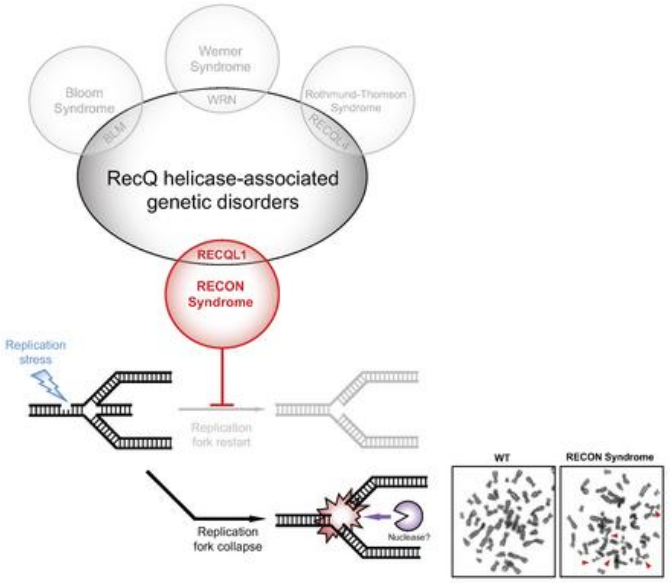

Find the latest version:

https://jci.me/147301/pdf

RECON syndrome is a genome instability disorder caused by mutations in the DNA helicase RECQL1

Bassam Abu-Libdeh[1*], Satpal S. Jhujh[2*], Srijita Dhar[3*], Joshua A. Sommers[3*], Arindam Datta[3], Gabriel M. C. Longo[4], Laura J. Grange[2], John J. Reynolds[2], Sophie L. Cooke[2], Gavin S. McNee[2], Robert Hollingworth[2], Beth L. Woodward[2], Anil N. Ganesh[2], Stephen J. Smerdon[2], Claudia M. Nicolae[5], Karina Durlacher-Betzer[6], Vered Molho-Pessach[7], Abdulsalam Abu-Libdeh[1], Vardiella Meiner[6], George-Lucian Moldovan[5], Vassilis Roukos[4], Tamar Harel[6#], Robert M. Brosh Jr.[3#], Grant S. Stewart[2#].

1. Department of Pediatrics & Genetics, Makassed Hospital & Al-Quds Medical School, E. Jerusalem, Palestine
2. Institute for Cancer and Genomic Sciences, University of Birmingham, Birmingham, United Kingdom
3. Translational Gerontology Branch, National Institute on Aging, National Institutes of Health, Baltimore, Maryland, USA
4. Institute of Molecular Biology (IMB), Mainz 55128, Germany
5. Department of Biochemistry and Molecular Biology, The Pennsylvania State University College of Medicine, Hershey, Pennsylvania, USA
6. Faculty of Medicine, Hebrew University of Jerusalem, Israel; Department of Genetics, Hadassah Medical Center, Jerusalem, Israel
7. Faculty of Medicine, Hebrew University of Jerusalem, Israel; Paediatric Dermatology Service, Department of Dermatology, Hadassah Medical Center, Jerusalem, Israel

* These authors have contributed equally

Correspondence: Grant S. Stewart (Email: g.s.stewart@bham.ac.uk; Tel: +121-414-9168), Robert M. Brosh Jr. (Email: broshr@mail.nih.gov; Tel:+410-558-8578), Tamar Harel (Email: tamarhe@hadassah.org.il; Tel: +972-2-6776329)

Conflicts of Interest Statement: The authors have declared that no conflict of interest exists.

Abstract

Despite being the first homolog of the bacterial RecQ helicase to be identified in humans the function of RECQL1 remains poorly characterised. Furthermore, unlike other members of the human RECQ family of helicases, mutations in RECQL1 have not been associated with a genetic disease. Here we identify two families with a novel genome instability disorder, named RECON (RECql ONe) Syndrome caused by biallelic mutations in the *RECQL* gene. The affected individuals exhibit short stature, progeroid facial features, a hypoplastic nose, xeroderma and skin photosensitivity. Affected individuals were homozygous for the same missense mutation in RECQL1 (p.Ala459Ser) located within its zinc binding domain. Biochemical analysis of the mutant RECQL1 protein revealed that the p.A459S missense mutation compromised its ATPase, helicase and fork restoration activity, whilst its capacity to promote single-strand DNA annealing was largely unaffected. At the cellular level, this mutation in RECQL1 gave rise to a defect in the ability to repair DNA damage induced by exposure to topoisomerase poisons and a failure of DNA replication to progress efficiently in the presence of abortive topoisomerase lesions. Taken together, RECQL1 is the fourth member of the RecQ family of helicases to be associated with a human genome instability disorder.

Introduction

DNA helicases are ubiquitous enzymes found in most uni- and multi-cellular organisms and function to unwind DNA in an ATP-dependent and direction-specific manner. The ability to unwind DNA is an essential step in many fundamental cellular processes, such as DNA replication, recombination, repair and transcription. The RecQ family of helicases represents one of the most highly conserved groups of 3´-5´ DNA helicases and is named after the prototype *Escherichia coli* RecQ. Whilst bacteria and yeast only express one RecQ-type helicase, higher eukaryotes possess multiple homologs, which are highly conserved. The RecQ helicase family has 5 known homologs in humans: RECQL (also known as RECQ1 or RECQL1), WRN, BLM, RECQL4 and RECQL5. Strikingly, biallelic mutations in three out five of these RecQ homologs, *WRN*, *BLM* and *RECQL4*, have been associated with rare genetic disorders in humans, characterised by chromosomal instability and cancer predisposition (1-2). Notably however, these genetic disorders are distinct with each syndrome exhibiting a unique set of clinical and cellular features. This serves to highlight that despite each of these enzymes being structurally and functionally related, they perform distinct tasks within the cell.

WRN is mutated in Werner Syndrome (WS), which is a progeroid syndrome associated with premature aging, type II diabetes, osteoporosis, cataracts, greying and loss of hair, skin atrophy and cancer predisposition. Cells from individuals with WS characteristically undergo premature replicative senescence associated with increased telomere erosion and have been reported to be hypersensitive to genotoxic agents that induce replication stress, such as camptothecin (CPT), methylmethane sulfonate (MMS) and G-quadruplex (G4) stabilisers (3). In contrast, Bloom Syndrome (BS), which is caused by mutations in *BLM*, is a developmental disorder typically presenting with microcephaly, short stature, immunodeficiency, skin hyper/hypopigmentation, photosensitivity, facial erythema and increased predisposition for developing cancer (4). The BLM helicase has been implicated in repairing DNA double strand breaks (DSBs), restarting damaged replication forks and resolving homologous recombination (HR) intermediates, including those present in mitosis as a result of under-replicated DNA transiting through the cell cycle (5). Consequently, cells devoid of BLM are hypersensitive to replication stress-inducing genotoxins such as CPT, hydroxyurea (HU) and aphidicolin (APH) and exhibit a characteristic increase in spontaneous sister chromatid exchanges (SCEs). Lastly, mutations in *RECQL4* have been associated with three distinct, albeit overlapping, genetic disorders: Rothmund-Thomson Syndrome (RTS), RAPADILINO, and Baller-Gerold Syndrome (BGS). Whilst patients with

each of these three disorders display some unique clinical features, e.g. poikiloderma (RTS) or craniosynostosis (BGS), the vast majority of affected individuals exhibit a constellation of developmental abnormalities, such as growth retardation, aplastic/absent thumbs, aplastic/absent patellae, aplastic/absent bones in the forearms, skin hypo/hyperpigmentation, cleft palate and also an increased predisposition for developing cancer (6). Unlike WRN or BLM, RECQL4 is a constitutive component of the replication machinery involved in regulating replication origin firing (7). However, RECQL4 has also been suggested to play a role in repairing oxidative base damage and DSBs by HR (8, 9). Accordingly, cells lacking RECQL4 function are hypersensitive to both DSB- and replication stress-inducing agents, e.g. ionising radiation (IR), CPT, HU and H_2O_2.

Despite RECQL1 being the first RecQ family helicase to be identified in humans, it remains the most functionally enigmatic (10). In vitro RECQL1 can unwind a variety of DNA structures in a 3´-5´ direction, particularly those with a 3´ single-stranded DNA tail, e.g. replication fork structures. It can also catalyse branch migration of Holliday junctions and D-loops, unwind G4 structures and promote single-stranded DNA annealing (SSA). However, unlike other human RecQ helicases it acts poorly to unwind RNA:DNA hybrids or displace Rad51 bound to single-stranded DNA (ssDNA) (11, 12). Despite its demonstrated biochemical activities, mice devoid of this enzyme are phenotypically normal (13). To date, there are reports suggesting that RECQL1 is required to repair DSBs induced by IR, CPT and etoposide (ETOP) (13,14), although the underlying mechanism is not clear. More recently, it has been proposed that a major function of RECQL1 is to promote the restart of stalled replication forks induced by the inhibition of topoisomerase 1 and that this activity is inhibited by poly-ADP-ribose polymerase 1 (PARP1), allowing the damaged forks time to repair (14). However, whether the role of RECQL1 in promoting the restart of reversed forks caused by abortive topoisomerase activity is solely dependent on PARP1 or whether RECQL1 plays a more fundamental role in this process remains to be clarified.

Whilst *RECQL* has not been previously associated with a defined human chromosomal instability disorder, mono-allelic germline mutations have been associated with a moderate increased risk for developing breast cancer (15, 16). Interestingly, Sun et al. (16) identified two *BRCA1/2* negative breast cancer families with missense variants in the zinc binding domain (ZBD) of RECQL1 (p.Arg455Cys and p.Met458Lys) that completely abolished its helicase activity. Moreover, functional analysis of conserved cysteine residues within this domain demonstrated that cysteine residues 453, 475 and 478 are critical for RECQL1 to hydrolyse ATP and unwind double-stranded DNA but not to

promote SSA (17). Combined, these observations serve to highlight the functional significance of the ZBD of RECQL1 and its importance in relation to its ability to act as a DNA helicase.

Here, we demonstrate that biallelic *RECQL* mutations are associated with a human genome instability syndrome, which we propose to name RECON (RECql ONe) Syndrome. Notably, individuals from both affected, but seemingly unrelated, families carry a homozygous missense mutation (p.Ala459Ser, referred to as p.A459S) in the ZBD of RECQL1. Clinically, this *RECQL* mutation is associated with a distinct disorder characterised by striking progeroid facial features, a tiny, pinched nose, apparent skin photosensitivity, xeroderma and slender, elongated thumbs. Functionally, the p.A459S mutation significantly compromised the ATPase/helicase activity of RECQL1 and modestly affected its ability to bind DNA. However, its capacity to promote SSA was unaffected. At the cellular level, this mutation gave rise to a modest defect in repairing abortive topoisomerase 1 (TOP1) and topoisomerase 2 (TOP2) cleavage complexes and a reduced ability to replicate in the presence of CPT/ETOP-induced DNA damage. Furthermore, cells expressing the p.A459S mutant RECQL1 also failed to efficiently restart replication following exposure to HU and MMS indicating that the role that RECQL1 plays in restarting damaged replication forks is not just limited to those associated with abortive TOP1/2 complexes. Taken together, these data suggest that whilst it is not essential (13), RECQL1 has non-redundant functions with other RecQ helicases and that its loss compromises genome stability and normal embryonic development.

Results

Clinical phenotype of individuals affected by RECQL1 mutations. Family A. The proband (Family A, III-2) was a female evaluated at age 9 years, 8 months for short stature, dysmorphism and dryness of skin and eyes. She was the second of five children born to parents of Middle Eastern descent, double first cousins (Figure. 1A). Pregnancy and delivery were uncomplicated. She was born at term with a birthweight of approximately 3000 grams. Developmental milestones, including motor, speech and communication skills, were age appropriate. At 18 months, medical evaluation was sought since her nose remained exceptionally small compared to the rest of her face, her eyes remained open while sleeping and she suffered from xerophthalmia (dry eyes) and xeroderma (dry skin) with scaling. Eruption of primary teeth was age appropriate. However, her permanent teeth were delayed in erupting. Parents reported photosensitivity. Physical examination at 9 years, 8 months revealed height 123.8 cm (Z score -1.98), weight 22.5 kg (Z score -2.05), and head circumference of 50 cm (Z score -1.64). A negative Z score represents the number of standard deviations below the population mean for each clinical measurement. Dysmorphic features included round face, redness of eyes, a tiny, pinched nose with anteverted nares, prominent premaxilla, and smooth philtrum (Figure. 1B). The proband's thumbs were slender and elongated, with hyperconvex nails. There was slight hyperextension of the elbows, but no joint laxity in the fingers. She had livedo reticularis and keratosis pilaris (Table 1).

A younger sister of the proband (Family A, III-4), examined at age 4 years, presented with similar clinical features. Pregnancy and delivery were uncomplicated, and developmental milestones were age appropriate. Physical examination revealed height of 96.4 cm (Z score -1.02), weight 13.9 cm (Z score -1.05) and head circumference 47.8 cm (Z score -1.18). She had dysmorphism including a somewhat aged (progeroid) appearance with little subcutaneous fat, red eyes, a tiny, pinched nose with anteverted nares, prominent premaxilla, and smooth philtrum (Figure 1B). Her thumbs were long and slender with proximal insertion, and she had mild hirsutism of the back. There was minor joint laxity of the fingers (Table 1). Family history was further positive for two common adult first cousins of the parents with similar clinical features. Unfortunately, these relatives were not available for genetic evaluation nor detailed medical work-up.

Family B. The proband (Family B, III-4) was a female, the fourth of six children born to parents of Middle Eastern descent with no known consanguinity (Figure 1A). She was referred for evaluation for the first time at the age of 5 years, 10 months for dysmorphism and dryness of skin. Pregnancy and

delivery were uncomplicated. She was born at term with a birth weight of 3500 grams. Developmental milestones, including motor, speech and communication skills, were age appropriate. Her other medical problems at that time were thrombocytopenia of undetermined cause and recurrent chest infections. Parents reported photosensitivity. Physical examination revealed height 110 cm (Z score -0.7), weight 13.5 kg (Z score -3.4), and head circumference of 47 cm (Z score -2.9). Dysmorphic features included a mask senile-like face (progeroid), deep set eyes, absent lower lid eyelashes, small ears with small, attached earlobes, prominent nasal bridge with a tiny, pinched nose with hypoplastic alae nasi, prominent premaxilla, thin lips and smooth philtrum (Figure 1B). There was bilateral arachnodactyly and thumbs were slender and elongated, with hyperconvex nails. She had hirsutism of the lower limbs, and there was thin dry skin (xeroderma) with areas of desquamation (scaling), mainly on exposed body parts suggestive of photosensitivity. She had thin extremities with hypoplastic muscles and subcutaneous fat. Follow-up measurements at age 14 years, 9 months revealed height 138.4 cm (Z score -3.59), weight 22.1 kg (Z score -8.47), and head circumference of 50.8 cm (Z score -2.92) (Table 1). Neither family reported any history of breast cancer or any other cancers. Genetic testing included chromosome analysis, chromosome breakage studies with diepoxybutane and Sanger sequencing for mutations in *ERCC6* and *ERCC8* were all normal.

Whole exome sequencing identified a homozygous missense mutation in RECQL. To identify the genetic cause of the disorder exhibited by Family A, whole exome sequencing was carried out on DNA derived from the proband (III-2) of Family A. After exclusion of non-authentic variants and inconsistent mutations, data mining identified a predicted pathogenic variant in *RECQL* (chr12:21626557[hg19]: NM_032941.2; c.1375G>T; p.Ala459Ser – referred to as p.A459S) as the primary candidate (Figure 1C). This variant affects a highly conserved alanine residue (GERP score 6.04) that lies within the ZBD of the RECQL1 protein (Supplementary Figure 1A-C). Moreover, this variant is not found in the gnomAD nor GME variome databases, nor in our local databases of ~10,000 exomes. It is predicted to be pathogenic by several bioinformatics algorithms including CADD (score 25.9), MutationTaster (score 1.0), Polyphen-2 (score 0.846), and DANN (score 0.9977). Notably, monoallelic alteration of the adjacent amino acid 458 (p.Met458Lys) has previously been linked with an increased predisposition for developing breast cancer. Moreover, functional studies of this mutation revealed that it significantly compromised the helicase activity of RECQL1 (14). Family B was identified due to the striking similarity

of clinical features exhibited by the proband (III-4) and the two affected siblings from Family A. Segregation analysis by Sanger sequencing of gDNA from both families confirmed segregation of this variant with the clinical phenotype (Figure 1A). All three affected individuals (III-2 and III-4 from Family A and III-4 from Family B) were homozygous for this variant, whereas available parents and eight healthy siblings were either heterozygous or wild type (LOD score (θ=0) was Z=3.311).

To determine what impact the p.A459S mutation had on RECQL1 protein stability, Western blotting was carried out on whole cell extracts generated from lymphoblastoid cell lines (LCLs) derived from RECQL1 patient III-2 from family A (RECQL1-P1-1) and RECQL1 patient III-4 from family B (RECQL1-P2). No obvious differences were observed in the expression of RECQL1 protein in LCLs from the two affected patients when compared to the expression of RECQL1 in LCLs from two normal individuals (Supplementary Figure 1C). Moreover, the p.A459S mutant RECQL1 protein localised normally to the nucleus in the presence or absence of DNA damage and was still able to associate with PARP1, a known RECQL1 binding protein (14) (Supplementary Figure 1D-1F). Therefore, to gain insight into the pathogenesis of RECON syndrome, we utilised biochemical and cell biological approaches to study the effects of the RECQL1 p.A459S mutation on its enzymatic activity and roles in regulating the cellular DNA damage response.

RECQL1-A459S displays significantly reduced DNA unwinding activity on a preferred forked duplex DNA substrate. Given that it had been previously shown that mutating the residue preceding alanine-459 (methionine-458) to a lysine abolished helicase activity (16), this prompted us to biochemically characterize RECQL1-A459S and compare its properties with wild type (WT) RECQL1. Initially, recombinant WT and mutant RECQL1 were expressed and purified from insect cells to near homogeneity (Figure 2A). Following this, using a 19-bp forked duplex as a substrate to measure its helicase activity, a simple protein titration of the wild type and mutant RECQL1 proteins revealed that the p.A459S mutation significantly reduced its helicase activity. At a protein concentration of 2.5 nM, RECQL1-WT unwound nearly 60% of the DNA substrate compared to approximately 20% for mutant RECQL1 (Fig 2B, 2C). To ascertain if the DNA unwinding by RECQL1-A459S was ATP-dependent, the mutant protein was incubated with the 19-bp forked duplex DNA substrate in the presence/absence of ATP. As predicted, RECQL1-A459S failed to unwind the DNA substrate when ATP was absent, consistent with the behaviour of RECQL1-WT (Figure 2D, 2E).

Kinetic analysis of RECQL1-dependent unwinding of the 19-bp forked DNA duplex showed a 2.6-fold reduction in the rate catalysed by the p.A459S mutant compared to WT at a protein concentration of 0.3 nM (Supplementary Figure 2A-C). Using a 4-fold greater concentration of RECQL1 protein (1.2 nM), the rate of helicase activity was reduced 4.8-fold for RECQL1-A459S (Figure 2F-H), suggesting that the reduction in the unwinding rate on the short 19-bp forked duplex was in part protein concentration dependent.

RECQL1, like the other human RecQ helicases, displays significantly compromised helicase activity on longer duplex DNA substrates, suggesting that the enzyme lacks processivity (18, 19). This led us to assess helicase-catalyzed DNA unwinding by the wild type and mutant RECQL1 proteins on a longer 31-bp forked duplex DNA substrate. As shown in Supplementary Figure 3A and 3B, RECQL1-A459S displayed significantly reduced helicase activity on the 31-bp forked duplex compared to RECQL1-WT. Approximately 3-fold less DNA substrate was unwound by RECQL1-A459S compared to RECQL1-WT at a protein concentration of 40 nM. This led us to perform a kinetic analysis of the WT and p.A459S RECQL1 proteins on the 31-bp forked duplex with two different concentrations of RECQL1. At 30 nM RECQL1 concentration there was a 3.8-fold difference in rate of unwinding (Supplementary Figure 3C-E). A similar reduction in rate of unwinding by the p.A459S mutant was observed at 40 nM RECQL1 protein concentration (Supplementary Figure 3F-H).

Altogether, the findings from these helicase studies demonstrate that the p.A459S amino acid substitution in the ZBD of RECQL1 compromises its DNA unwinding activity, a result that is consistent with previous studies assessing the impact of other RECQL1 ZBD mutations on its helicase activity (16, 17).

p.A459S RECQL1 poorly restores a replication fork from its regressed state. Since RECQL1 has been previously shown to restore replication forks that have been regressed (14), we used a reversed fork structure (Figure 3A) as a substrate in our in vitro RECQL1 enzymatic assays to assess whether the p.A459S mutation affected the ability of RECQL1 to remodel a reversed fork. Over a 30-min time course, the p.A459S mutant RECQL1 consistently displayed a reduced ability to restore the replication fork compared to RECQL1-WT (Figure 3B, 3C). We observed as much as a 7-fold difference in fork restoration at the 5-min time point and at least a 3.5-fold difference at later time points in the reaction (Figure 3B, 3C). Interestingly, we also detected a small but detectable amount of helicase activity using

the reversed fork structure as a substrate (Figure 3B), which was also reduced by the p.A459S mutation. This indicates the p.A459S mutation not only compromises the ability of RECQL1 to unwind fork duplexed DNA structures but also to remodel reversed forks in vitro.

RECQL1-A459S retains SSA activity comparable to RECQL1-WT. Purified human recombinant RECQL1 protein is also known to display potent strand annealing activity (19). To address whether this activity is also affected by the p.A459S mutation, we examined the ability of mutant and wild type RECQL1 proteins to anneal two partially complementary oligonucleotides to form a 19-bp forked DNA duplex. These experiments were performed in the absence of ATP to prevent helicase-catalyzed unwinding of the annealed forked duplex, which would normally serve as a canonical substrate for the RECQL1 helicase activity. As shown in Figures 3C and 3D, the strand annealing activity of WT and mutant RECQL1 proteins were near identical over a range of protein concentrations indicating that despite the compromised helicase activity of RECQL1-A459S, its strand annealing activity remains intact.

RECQL1-A459S displays modestly reduced DNA substrate binding compared to RECQL1-WT. Given that RECQL1-A459S has reduced helicase but proficient strand annealing activity compared to RECQL1-WT, we wanted to examine their relative DNA binding capacities using EMSA, a sensitive technique that allows both visual evidence and quantitative assessment of nucleic acid binding. Although RECQL1 binds to various DNA substrates, it has been shown to preferentially bind a forked DNA duplex molecule over single-stranded or fully duplexed DNA molecules (11, 19). Therefore, we chose to study the DNA binding capabilities of wild type and mutant RECQL1 proteins using the 19-bp forked duplex DNA substrate we had tested in the helicase assays. In this case, we omitted ATP or included ATPγS in the binding mixtures to prevent helicase activity. From these assays, it was observed that both mutant and wild type RECQL1 proteins could bind the forked duplex DNA molecule, shifting the free radiolabelled DNA to three specific slower migrating bands presumably representing the DNA substrate bound by monomer and multimeric species (Supplementary Figure 4A, 4B). However, quantitative assessment of the DNA binding isotherm data from binding incubations conducted in the absence of ATP indicated a 1.5-fold greater apparent dissociation constant (K_d) for RECQL1-A459S compared to RECQL1-WT (Supplementary Figure 4A), suggesting a modest decrease in the affinity of

RECQL1-A459S for the forked duplex DNA compared to RECQL1-WT. We observed a similar increase of 1.4-fold in the K_d value for RECQL1-A459S in the presence of ATPγS when compared to WT (Supplementary Figure 4B).

To further study the apparent difference in DNA binding between RECQL1-WT and RECQL1-A459S, we performed DNA binding assays in which a competitor oligonucleotide was used as a challenging agent after pre-incubation of the RECQL1 protein with the radiolabeled forked duplex DNA molecule (Supplementary Figure 5A). Both the mutant and WT RECQL1 proteins showed a similar reduction in DNA binding with increasing concentration of unlabelled competitor (Supplementary Figure 5B, 5C), suggesting that the stability of the pre-formed forked duplex-RECQL1 protein complex was similar for the wild type and mutant forms of RECQL1.

Effect of the RECQL1-A459S mutation on kinetic parameters for ATP hydrolysis. To determine the ability of RECQL1-A459S to bind and hydrolyze ATP, we conducted a series of ATPase assays to measure the k_{cat}, K_m and V_{max} for ATP hydrolysis. In kinetics assays with an ATP concentration of 1 mM, RECQL1-WT had almost a 3-fold higher k_{cat} for ATP hydrolysis in the presence of M13mp18 ssDNA effector compared to RECQL1-A459S (Table 2). In ATPase assays with varying ATP concentrations, RECQL1-WT had a 3-fold greater maximum velocity (V_{max}) and a 2-fold greater K_m compared to RECQL1-A459S (Table 2), suggesting that the diminished turnover of ATP catalysed by the RECQL1-A459S mutant is not reflected by reduced nucleotide binding.

RECQL1-A459S protein retains its ability to oligomerize. To examine the effect of the RECQL1-A459S mutation on its ability to oligomerize, we performed size exclusion chromatography. As seen in previous studies (20, 21), the RECQL1-WT protein eluted from the column in two distinct peaks in the absence of ATP (Supplementary Figure 6). The RECQL1-A459S protein also eluted as two peaks at similar volumes indicating that the mutant protein behaves similar to RECQL1-WT.

The hypomorphic p.A459S RECQL1 mutation causes a defect in the repair of abortive TOP1/2 lesions. Since RECQL1 has been previously shown to be important for the repair of DNA damage caused by poisoning TOP1/2 (14, 22) and that the p.A459S mutation significantly compromises the helicase activity of RECQL1 (this study), it was conceivable that cell lines derived from the affected patients

would exhibit aberrant repair of DNA breaks induced by exposure to CPT and ETOP. To investigate this, a skin fibroblast cell line was derived from patient III-2 from Family A (named RECQL1-P1-1), immortalised with hTERT and complemented with either an empty vector, or a vector expressing WT or p.A459S mutant RECQL1. Expression of the exogenous RECQL1 was verified by Western blotting (Supplementary Figure 7A). Following this, the cell lines were exposed to low dose CPT or ETOP for a short period of time and then incubated in drug free media to allow time for repair to occur. To monitor DNA DSB induction and repair, 53BP1 foci were quantified over a 24 h time course (Figure 4A, Supplementary Figure 7B). Consistent with a role for RECQL1 in repair of TOP1/2-associated DSBs, patient cells expressing either the empty vector or the p.A459S mutant RECQL1 exhibited greater levels of 53BP1 foci in cells throughout a 24 h time course following exposure to CPT or ETOP than cells expressing WT RECQL1, despite equal levels of DNA damage being induced in all three cell lines and no obvious differences in cell cycle profile being observed throughout the time course (Figure 4A, Supplementary Figure 7C). Interestingly, even in the absence of DNA damaging agents, cells containing the empty vector or expressing the p.A459S RECQL1 mutant exhibited higher levels of spontaneous 53BP1 foci compared to cells expressing WT RECQL1 (Figure 4A, Supplementary Figure 7B). To validate these observations further, we quantified the formation of micronuclei as a marker of genome stability in all three cell lines before and after exposure to CPT or ETOP. In keeping with the 53BP1 quantification, cells containing the empty vector or expressing p.A459S mutant RECQL1 exhibited significantly greater levels of spontaneous and CPT/ETOP-induced micronuclei than their WT RECQL1 expressing counterpart does (Figure 4B). Consistent with this, RECQL1 CRISPR knockout HeLa cells complemented with empty vector or mutant RECQL1 exhibited a similar increase in residual 53BP1 foci and micronuclei 24 h following exposure to CPT or ETOP when compared to knockout cells complemented with WT RECQL1 (Supplementary Figure 8A-C). However, under the growth conditions used within this study, RECQL1 knockout HeLa cells did not display a significant hypersensitivity to either CPT or ETOP as assessed by colony survival assay (Supplementary Figure 8D, 8E), suggesting that more sensitive methods of measuring DNA damage repair are required to assess the impact of RECQL1 deficiency on genome stability.

To assess more directly what affect the p.A459S RECQL1 mutation had on DNA repair and genome stability, we quantified chromosome breakage by analysis of metaphase spreads from LCLs derived from patients RECQL1-P1-1 and RECQL1-P2. In keeping with our previous observations

quantifying 53BP1 foci, the RECQL1-P1-1 and RECQL1-P2 LCLs exhibited higher levels of spontaneous and CPT/ETOP-induced chromosome breakage than two normal LCLs. Notably, the chromosome breakage phenotype observed in the two RECQL1 mutant LCLs was comparable to that exhibited by an LCL derived from an Ataxia Telangiectasia-Like Disorder (ATLD) patient carrying a hypomorphic homozygous truncating mutation in *MRE11A* (22) following exposure to CPT but was significantly lower than the ATLD cell line following exposure to ETOP (Figure 4C). A similar pattern was observed when quantifying spontaneous and CPT/ETOP-induced chromosome radial/exchanges in these cell lines (Supplementary Figure 9A). Importantly, both the increased spontaneous and CPT/ETOP-induced chromosome breakage were also observed in fibroblasts from patient RECQL1-P1 and could be complemented by expression of exogenous WT but not mutant A459S RECQL1 (Figure 4D).

Whilst the precise mechanism in which RECQL1 functions to mediate DSB repair is unclear, several reports have suggested that like other RecQ helicases, RECQL1 regulates HR by affecting the interaction of the strand exchange protein, Rad51, with DNA during repair (13,23). To ascertain whether the underlying DNA repair defect in patient-derived cell lines could be caused by aberrant regulation of Rad51, the isogenic complemented fibroblasts were exposed to CPT or ETOP, fixed and then stained with antibodies to Rad51 and mitosin (a marker of S/G2 cells). Quantification of Rad51 foci in S/G2 cells by fluorescence microscopy revealed that whilst the cells containing an empty vector or expressing mutant RECQL1 exhibited a greater level of spontaneous Rad51 than the cells complemented with WT RECQL1 (Supplementary Figure 9B), there was no difference in the percentage of S/G2 cells with >10 Rad51 foci following exposure to either CPT or ETOP at both early and late time points between the three cell lines (Supplementary Figure 9C). Consistent with the increased spontaneous Rad51 foci in the RECQL1 mutant fibroblasts, LCLs derived from both RECQL1-P1-1 and RECQL1-P2 both exhibited a mild increase in spontaneous and DNA damage-induced sister chromatid exchanges (Supplementary Figure 9D). Similar observations were reported for *Recql* knockout mouse embryo fibroblasts exposed to ionising radiation (13). Importantly, this phenotype was recapitulated in the RECQL1 CRISPR knockout HeLa cells and could be complemented by re-expression of WT but not p.A459S mutant RECQL1 (Supplementary Figure 9E). Taken together, these results suggest that the defective repair of CPT- or ETOP-induced DNA damage may arise either because of defective DNA damage response (DDR) signalling and/or an inability of the replisome to progress past these lesions, resulting in under-

replicated DNA transiting through the cell cycle into the following G1 phase. To investigate the first possibility, LCLs from two normal individuals and the two affected RECQL1 mutant patients (RECQL-P1-1 and RECQL1-P2) were transiently exposed to CPT or ETOP and following the induction of DNA damage, early and late time points were taken to examine the activation of the DDR by Western blotting using phospho-ATM, SMC1, Nbs1, Chk1, RPA2 and H2AX as markers. Despite some mild variability in the level of the DNA damage response induced by CPT or ETOP, both RECQL1 mutant cell lines exhibited robust activation of the ATM-dependent DDR (Supplementary Figure 10), suggesting that defective DDR signalling is not the underlying cause of compromised repair of CPT/ETOP-induced DNA lesions in RECQL1 mutant cells.

An inability to repair TOP2-associated DSBs in cells derived from RECON syndrome patients does not compromise the induction or repair of DSBs within MLL locus. It is known that TDP2, MRE11 and components of the NHEJ DSB repair pathway are critical for repair of TOP2-induced DSBs, especially within the *MLL* locus, which frequently undergoes chromosomal translocation if mis-repaired (24, 25). Given the inability of cells from RECON syndrome patients to efficiently repair ETOP-induced DSBs, we sought to investigate whether the hypomorphic p.A459S RECQL1 mutation present in these cells was associated with aberrant repair of DSBs within the *MLL* locus. Utilising C-Fusion 3D, a high-throughput imaging methodology to probe chromosomal breakage and rare translocations in single cells (25), we exposed two normal LCLs, LCLs from a TDP2 mutant patient and the two RECON syndrome patients to etoposide and monitored *MLL* locus breakage and translocation to the *ENL* locus. Notably, whilst the TDP2 mutant LCL displayed a high frequency of breakage of the *MLL* gene locus and translocation to the *ENL* locus following exposure to etoposide, this was not observed in either RECQL1 mutant LCLs (Supplementary Figure 11A, 11B). These results suggest that RECQL1 does not play a major role in the repair of TOP2-dependent DSBs located within the *MLL* locus.

Cells from RECON syndrome patients exhibit a reduced ability to replicate in the presence of abortive topoisomerase lesions. It was reported that RECQL1 is required to restart stalled replication forks following the pharmacological inhibition of TOP1 and that cells lacking RECQL1 activity accumulate reversed forks in the presence of CPT (14). To investigate the impact of the RECQL1 p.A459S mutation on replication, we carried out DNA fibre analysis using LCLs from the affected RECQL1 patients in the

presence or absence of CPT or ETOP. Interestingly, even in the absence of exposure to genotoxins, both RECQL1 LCLs displayed an increase in spontaneously stalled forks indicative of higher levels of endogenous replication stress (Figure 5A). Whilst our analysis cannot distinguish between stalled and reversed forks as they would both give rise to CldU-only fibres, it is plausible that our observations are consistent with a previous study demonstrating that depletion of RECQL1 results in an increase in reversed forks even in the absence of exogenously induced DNA damage (26, 27). Following exposure to either CPT or ETOP, our DNA fibre analysis also revealed that both RECQL1 mutant patient cell lines were unable to efficiently replicate in the presence of abortive TOP1 or TOP2-induced DNA lesions, despite the lack of gross alterations in replication fork speed or new origin firing prior to treatment (Figure 5C, Supplementary Figure 12A, 12B). Notably, both the spontaneous and CPT/ETOP-induced replication phenotypes were also observed in the patient-derived fibroblasts and could be complemented by the expression of WT but not mutant p.A459S RECQL1 (Figure 5B, 5D, Supplementary Figure 12C, 12D). Taken together, these data suggest that the clinically relevant p.A459S mutation in the RECQL1 ZBD, which perturbs its catalytic activity, compromises the ability of RECQL1 to restart reversed replication forks.

Cells from individuals with RECON syndrome exhibit an reduced ability to efficiently restart HU- and MMS-damaged replication forks. It was previously determined that RECQL1, like other helicases such as WRN (26), DNA2 (26) and BLM (28), RECQL1 plays a role in promoting the restart of HU-stalled forks (29). To investigate whether the RECON syndrome patient-derived cell lines exhibit a global inability to restart replication forks that is not just restricted to forks stalled by abortive topoisomerase cleavage complexes, DNA fibre analysis was carried out with RECQL-P1-1 complemented fibroblasts following a transient exposure to high dose HU. Interestingly, this analysis demonstrated that the p.A459S mutation significantly compromised the ability of replication forks transiently stalled by HU to restart efficiently (Figure 6A). Importantly, this phenotype was also recapitulated in the RECQL1 CRISPR knockout HeLa cells complemented with either an empty vector or the p.A459S RECQL1 mutant (Supplementary Figure 12E). Furthermore, the efficiency of replication progression for those forks that did manage to restart following release from HU was also severely affected in the RECQL-P1-1 fibroblasts complemented with empty vector or the p.A459S mutant as compared to those complemented with WT RECQL1 (Figure 6B). These data suggest that RECQL1 may be important for

the restart of all types of stalled replication forks irrespective of the causative DNA lesion. In keeping with this, the p.A459S mutant also compromised the ability of cells to restart replication in the presence of DNA alkylation damage induced by MMS exposure, accompanied by increased chromosome breakage and cell death (Supplementary Figure 13).

Lastly, it has been suggested RECQL1, in a manner similar to that of WRN and DNA2 (26), also functions to protect stalled forks from uncontrolled nucleolytic degradation. Therefore, to address whether the inability of the p.A459S mutant RECQL1 protein to efficiently restart HU-stalled forks is due to excessive fork degradation, the three isogenic complemented fibroblast cell lines were sequentially labelled with CldU and IdU and then exposed to 4 mM HU for 5 h. Replication fork stability was then quantified by calculating the ratio of CldU:IdU labelled fibres. As shown in Figure 6C, RECQL-P1-1 fibroblasts complemented with empty vector and the p.A459S exhibited a mild increase in replication fork degradation following prolonged exposure to HU exposure that could be complemented following the expression of WT RECQL1. This suggests that the replication fork restart defect present in the RECON syndrome derived patient cells is not only due to an inability of the mutant RECQL1 to remodel reversed forks but also results from stalled forks being degraded.

Discussion

Despite *RECQL* being cloned over 25 years ago (10), the role that it plays within the cell to maintain genome stability remains relatively unclear. In contrast, functional insight into how other RecQ helicase family members, such as BLM, WRN and RECQL4, protect the genome from deleterious DNA damage has been greatly facilitated by the identification of human disorders caused by mutations in these respective genes. However, even with the rapid advances in whole exome/genome sequencing technology, mutations in the two remaining RecQ helicase genes (*RECQL* and *RECQL5*) have yet to be linked to an inherited chromosomal instability syndrome. Here we describe the identification of a human chromosomal instability disorder, named RECON syndrome (RECql ONe), caused by biallelic missense mutations in *RECQL*. Notably, whilst it has been suggested that the function of RECQL1 may be redundant with other RecQ helicases such as BLM (30), the individuals affected by the RECQL1 p.A459S mutation exhibit a clinical phenotype distinct from BS, WS and the three RECQL4-associated disorders, suggesting that RECQL1 is not redundant with WRN, BLM or RECQL4 and performs unique functions during human development.

Whilst individuals with BS or one of the RECQL4-associated disorders are clinically distinguishable, they do exhibit an overlap of symptoms, such as pre- and post-natal growth retardation, facial erythema that worsens upon sun exposure, poikiloderma, skin hypo- and hyper-pigmentation, alopecia and an increased predisposition for developing cancer, which is probably reflective of common cellular processes that the encoded proteins have been reported to take part in e.g. DSB end-resection and DNA replication (8, 29, 31, 32). In comparison to the clinical features of BS, RTS, RAPADILINO and BGS, RECON syndrome patients only share post-natal growth retardation, despite RECQL1 also being implicated in regulating DSB repair and processing replication intermediates (14, 26, 28, 33).

In contrast, individuals with BS can be differentiated by the presence of microcephaly, immunodeficiency and type 2 diabetes, whereas patients with a RECQL4-associated disorder can be identified by the presence of absent/hypoplastic thumbs, radial ray defects, absent/hypoplastic patellae, limb malformations, cataracts, a reduced bone density, anaemia, neutropenia and craniosynostosis.

It appears that the defining features of RECON syndrome include skin photosensitivity, xeroderma, and a progeroid-like facial appearance with a tiny, pinched nose and prominent premaxilla define this genetic disorder clinically. Interestingly, the progeroid-like facial appearance, growth retardation and muscle wasting is somewhat reminiscent of WS and although it is likely that the affected

patients are currently too young to ascertain whether they exhibit any other clinical signs of premature aging, it is tempting to speculate that this represents another progeroid syndrome (34, 35).

Whilst it is apparent that the clinical phenotype exhibited by the affected individuals carrying *RECQL* mutations is relatively mild when compared to other RecQ-associated disorders, it should be noted that these individuals are not null and that the severity of the resulting clinical symptoms are likely to be tempered by the presence of some residual protein function. In addition, it is possible that some of the features of the disease are specific to this particular *RECQL* mutation and/or are modified by the similar genetic background of the two affected families. As such, the range and severity of the clinical symptoms linked with RECQL1 dysfunction will only be properly determined following the identification of additional patients. In relation to this, it has been reported by two laboratories that heterozygous mutations in *RECQL* are associated with an increased risk of developing breast cancer (15, 16). Although, this association has been disputed by several other groups (36, 37). Interestingly, one of the identified breast cancer-associated variants in *RECQL* altered the amino acid residue proximal to the RECON syndrome *RECQL* mutation. Despite this, none of the heterozygous carriers of the p.A459S mutation in either family A or B have reported the development of breast cancer. Thus, it is plausible that this *RECQL* variant might not be associated with an increased cancer predisposition, albeit that the carrier frequency for the p.A459S mutation is extremely low. However, since we have not directly compared the pathogenic impact of the syndrome and cancer-associated mutations in *RECQL* on its enzymatic activities and roles in regulating DNA replication, we acknowledge that it is difficult to make any conclusions regarding whether the p.A459S mutation may predispose to developing breast cancer. As such, further studies to address the genotype-phenotype relationship linking the molecular, cellular and clinical characteristics of individual RECQL1 mutations are warranted.

It has been suggested that the main function of RECQL1 is to promote the restart of reversed replication forks induced by abortive TOP1-cleavage complexes, which in turn is inhibited via an interaction of RECQL1 with PARP1 (14, 26). Interestingly, we detected a replication defect in RECON syndrome patient cells by DNA fibre analysis following the pharmacological inhibition of either TOP1 or TOP2 without a requirement to suppress PARP1 activity. This suggests that RECQL1 plays a more prominent role in regulating replication fork restart in the presence of abortive topoisomerase complexes than perhaps thought and that this function is only partly dependent on PARP1.

RECQL1's ability to restart forks through branch migration of a reversed fork was shown to require its ATPase activity (14). Whilst the p.A459S mutation lies outside of the RECQL1 helicase domain, it has been previously demonstrated that mutating conserved cysteine residues within the ZBD compromises both its ATPase and DNA unwinding activities (11, 12). In keeping with this, we have shown the p.A459S mutation also significantly reduces the ATPase, DNA unwinding and branch-migrating activities of RECQL1. Examination of available crystal structures of human RECQL1 show that the ZBD is spatially juxtaposed with the helicase ATP-binding cleft, which is located between the two N-terminal domains (Figure 7A). Interestingly, A459 contacts F281 located within the linker region between the two helicase domains that appears to adopt two conformations in the GDP-bound structure (40), one of which packs directly against P114 within the P-loop/Walker A/Motif1 region. Since A459 itself forms part of a hydrophobic cluster within the ZBD core that is likely perturbed by mutation to a more polar and bulkier serine residue, the presence of the serine residue may affect the ability of F281 to adopt these different conformations, thus potentially offering a molecular explanation for the effects of the p.A459S mutation on both ATPase and helicase activity (Figure 7B, 7C). In a manner similar to the RECQL1 p.A459S mutation, disease-causing missense mutations in the ZBD of BLM also compromise its ATP hydrolysis and DNA unwinding activities (38, 39). However, unlike RECQL1, BLM also contains a helicase and RNase C-terminal (HRDC) domain, which is required for Holliday junction dissolution (41). Therefore, even though pathogenic missense mutations have been identified in the conserved ZBD of BLM and RECQL1, the functional impact and clinical consequences of these mutations are likely to be distinct due to the unique structural architecture of the respective RecQ helicases.

Taken together, it is likely that the replication defects we observed in RECON syndrome derived patient cells are attributed to an inability of RECQL1 to restart reversed forks due to compromised ATP-dependent helicase/branch-migration activity. Fork reversal is thought to be a ubiquitous response to most types of replication stress and is essential for both the repair and restart of damaged replication forks. Therefore, if RECON syndrome represents a disease of failed replication restart, it is not clear why the clinical symptoms exhibited by the affected patients do not have more of a developmental component, e.g. similar to those of patients with Schimke imuno-osseous dysplasia (SIOD), which is caused by mutations in the fork remodelling factor, SMARCAL1 (42, 43). This suggests that perhaps

the fork restart function of RECQL1 is essential in some cell types but not others or is restricted to a subset of forks.

Interestingly, in addition to RECQL1, other disease-associated DNA helicases involved in replication fork processing and homologous recombination, such as DNA2, WRN, BLM, FANCJ and FANCM (44), have also been implicated in suppressing the nucleolytic degradation of stalled replication forks and promoting their restart once repaired. Notably, of these, the cellular replication response to CPT and HU damage in cells lacking WRN is most similar to those observed in the RECON syndrome cells i.e. both RECON syndrome and WS cells display increased fork degradation and a reduced efficiency with which replication can proceed in the presence of abortive TOP1 complexes or following HU exposure (26, 45). The similar cellular phenotypes of WS and RECON cells may reflect the progeroid-like features of both disorders. However, the increased severity of clinical symptoms exhibited by individuals with WS when compared to RECON syndrome may arise as a consequence of loss of specific enzymatic activities and/or functions of the WRN protein e.g. the exonuclease activity, that are not conserved in RECQL1. In this regard, it remains to be determined whether RECQL1 also plays a role in promoting telomeric replication by dissembling G-quadruplex structures or repairing oxidative damage in a manner similar to WRN.

In summary, we demonstrate that mutations in *RECQL* are the underlying cause of an inherited chromosomal instability syndrome, which exhibits some clinical and cellular phenotypic similarities with WS. Thus, RECQL1 represents the fourth RecQ helicase to be implicated in genetically inherited disease characterized by genome stability defects.

Methods

Exome analysis. Following informed consent, exome analysis was carried out using DNA extracted from whole blood of the proband in Family A (Figure. 1A). Exonic sequences from DNA were enriched with the Agilent V5 Kit (Agilent Technologies). Sequences were generated on a HiSeq2500 (Illumina) as 125-bp paired-end runs. Read alignment and variant calling were performed with DNAnexus (Palo Alto) using default parameters with the human genome assembly hg19 (GRCh37) as reference. Exome analysis of the proband yielded 60.95 million reads, with a mean coverage of 88.83×.

*Segregation analysis***.** An amplicon containing the *RECQL* variant was amplified by conventional PCR of genomic DNA derived from the probands and all available parents and siblings. PCR amplicons were analysed by Sanger sequencing. The genomic DNA primer sequences used for *RECQL* PCR amplification were: RECQL_F: 5'-TTAGCCTATAAAGGTTTACAAAACA-3'; RECQL_R: 5'-GGTAATATTATGGCAGTTATAGGAAGC-3'. The primers used to sequence *RECQL* cDNA were: RECQL_F: 5'-TGCAGGTCGAGATGACATGA-3'; RECQL_R: 5'-AGCATGTTTGCAGCCTTCTTC-3'.

Data Availability: The ClinVar accession number for the *RECQL* gene variant data is SCV001364447.1

Cell culture and generation of cell lines. Dermal primary fibroblasts were grown from skin-punch biopsies and maintained in Dulbecco's modified Eagle's medium (DMEM; Thermo Fisher) supplemented with 20% FCS, 5% L-glutamine and 5% penicillin-streptomycin (Merck) antibiotics. Primary fibroblasts were immortalized with a lentivirus expressing human telomerase reverse transcriptase (hTERT) that was generated by transfecting 293FT cells (Thermo Fisher) with the plasmids: pLV-hTERT-IRES-hygro (Addgene #85140), psPax2 (Addgene #12260) and pMD2.G (Addgene #12259). Selection was performed using Hygromycin (Thermo Fisher) at 70 µg/ml. All LCLs were routinely grown in RPMI-1640 (Thermo Fisher) supplemented with 10% FCS, 5% L-glutamine and 5% penicillin-streptomycin. *RECQL* knockout HeLa cells were routinely grown in DMEM supplemented with 10% FCS, 5% L-glutamine and 5% penicillin-streptomycin. Fibroblast and HeLa cell complementation was carried out using the pLVX-IRES-Neo lentiviral vector (Takara Bio) encoding 2xHA-tagged *RECQL*. All cell lines were routinely tested for mycoplasma.

Genotoxic agents. Camptothecin (Merck), etoposide (Merck), hydroxyurea (Sigma) and methylmethane sulfonate (Sigma) were used as indicated.

Immunoblot analysis, immunoprecipitation and antibodies. Whole-cell extracts were prepared and subjected to immunoblotting as previously described (23). Immunoblotting was performed using antibodies to: pS1981 ATM (AF1655) from R&D systems; ATM (A300-299A), pS824-KAP1 (A300-767A), KAP1 (A300-274A), pS966-SMC1 (A300-050A), SMC1 (A300-055A), pS4/S8-RPA2 (A300-245A) and RECQL1 (A300-450A) from Bethyl Laboratories; pS345-CHK1 (2341) from Cell Signalling Technology; CHK1 (sc-8408) and PARP1 (sc-8007) from Santa Cruz, H2A (07-146); γ-H2AX (05-636), RPA2 (NA18) and HA (H9658) from Merck; pS343-NBS1 (47272) from Abcam; Nbs1 (GTX70224) from GeneTex. Co-immunoprecipitation was carried out as previously described (23), with the exception that EDTA was excluded and 250 units/ml benzonase (Merck) and 1.5 mM $MgCl_2$ were added to the lysis buffer. 5 μg of anti-RECQL1 antibody (A300-450A) or a non-specific IgG (Dako) coupled with protein A-agarose beads (GE Healthcare) were used for isolating protein complexes from 5 mg of whole cell extract.

Immunofluorescence microscopy. Cells were seeded onto coverslips 24 h before extraction and fixation. 2 μg/ml cytochalasin B (Sigma) was added to the media for 24 h for the detection of micronuclei. Cells were pre-extracted for 5 min on ice with ice-cold buffer (25 mM HEPES, pH 7.4, 50 mM NaCl, 1 mM EDTA, 3 mM $MgCl_2$, 300 mM sucrose and 0.5% Triton X-100) and then fixed with 4% paraformaldehyde for 10 min. Fixed cells were stained with primary antibodies specific to γ-H2AX (Merck, 05-636), RAD51 (Merck, PC130), 53BP1 (Novus-Biologicals, NB100-904), RECQL1 (Abcam, Ab151501) and mitosin (BD Transuction labs, 610768) with secondary antibodies conjugated to Alexa Fluor 488 and Alexa Fluor 594 (Life Technologies), and then with DAPI (VectaLabs). Images were visualized using a Nikon Eclipse Ni microscope with NIS-Elements software (Nikon Instruments) and captured using a 100× oil-immersion objective.

DNA-fibre-spreading assay. Cells were pulse-labelled with 25 μM CldU for 20-30 min, washed with PBS, pulse-labelled with 250 μM IdU with or without 50 nM CPT or 50nM ETOP 20-30 min, and then harvested. For replication restart experiments, cells were labelled with CldU, washed in warm PBS,

incubated in media containing 2 mM HU or 0.02% MMS for 2 h or 20 min respectively. Cells were washed again in warm PBS and then incubated with IdU for the indicated time. DNA fibre analysis was carried out as previously described (46).

Metaphase spreads. Giemsa-stained metaphase spreads were prepared as previously described (46). Briefly, Colcemid (KaryoMAX, Thermo Fisher) was added at a final concentration of 0.2 µg/ml for 3 h. Cells were then harvested by trypsinization, subjected to hypotonic shock for 30 min at 37 °C in hypotonic buffer (10 mM KCl, 15% FCS) and fixed in 3:1 ethanol:acetic acid solution. Cells were dropped onto acetic-acid-humidified slides, stained for 15 min in Giemsa-modified solution (Merck; 5% vol/vol in water) and washed in water for 5 min before being visualised by light microscopy.

DNA helicase assays. DNA helicase assays were performed as previously described (19). Briefly, reactions were carried out in a 20 µl volume with 20 mM Tris (pH 7.4), 10 mM KCl, 5 mM ATP, 5 mM $MgCl_2$, 10% glycerol and 80 ng/µl BSA for 15 min at 37 °C. Reaction mixtures containing a forked duplex DNA substrate (19-bp or 31-bp) were incubated with the indicated concentrations of RECQL1-WT or RECQL1-A459S helicase proteins, as specified. Reactions were quenched with an equal volume of 2× stop dye (18 mM EDTA, 0.6% SDS, 25% glycerol, 0.4% bromophenol blue, 0.4% xylene cyanol and 0.1 mg/ml proteinase K) and incubated an additional 15 min at 37 °C to remove bound RECQL1 protein. Reaction products were resolved by electrophoresis on native 12% polyacrylamide gels at 200 V for 1.5 h. Radiolabeled DNA products were visualized with a phospho-imager and quantified using ImageQuant. For kinetic analysis of DNA unwinding, 19-bp or 31-bp forked duplex DNA substrates were incubated with the specified RECQL1 concentration and incubated for the indicated periods of time at 37 °C. Rates of helicase-catalyzed DNA unwinding were determined by linear regression analysis.

Strand annealing assays. Strand annealing assays were performed as previously described (19). Briefly, the specified concentration of RECQL1-WT or RECQL1-A459S helicase protein was incubated with 0.5 nM each of 5′-end radiolabeled oligonucleotide and partially complementary unlabeled oligonucleotide. Strand annealing reactions (20 µl) were carried out in helicase reaction buffer (20 mM Tris-HCl (pH 7.5), 10 mM KCl, 8 mM dithiothreitol, 5 mM $MgCl_2$) and quenched by addition of an equal

volume of 2X stop dye (18 mM EDTA, 0.6% SDS, 25% glycerol, 0.4% bromophenol blue, 0.4% xylene cyanol and 0.1 mg/ml proteinase K) and incubation for an additional 15 min at 37 °C to remove bound RECQL1 protein. Reaction products were electrophoresed on native 12% polyacrylamide gels at 200 V for 1.5 h. Radiolabeled products were visualized and quantified as described above.

Fork Restoration Kinetics Assay. 20 nM WT or A459S RECQL1 was incubated with 2 nM radiolabelled reversed fork substrate, 2 mM ATP, 15 mM phosphocreatine, and 30 u/ml creatine phosphokinase in reaction salts (35 mM Tris-HCl, pH 7.5, 20 mM KCl, 5 mM $MgCl_2$, 0.1 mg/ml BSA, 2 mM DTT, 5% glycerol) in 100 µl reactions at 37 °C. 20 µl aliquots were removed at the indicated times and were quenched by the addition of 10 µl of 3X stop buffer (1.2% SDS, 30% glycerol and Proteinase K) followed by incubation for at least 10 min at RT. Separate reactions containing either a reversed fork and replication fork structure without RECQL1 were incubated for 30 min at 37 °C followed by the addition of the 3X stop buffer. Samples were immediately loaded onto an 8% polyacrylamide 1X TBE gel and electrophoresed for 4 h at 200 V at 4 °C. Gels were exposed to a phospho-imager screen overnight and then imaged using a Typhoon FLA 9500 imager (Cytiva). Gel images were quantified using ImageQuant TL software (Cytiva) and raw data were processed in excel. The percentage fork restoration was calculated by dividing the volume of the replication fork band by the total volume at each time point and subtracting the percentage fork restored in the no enzyme control from each time point. Data representing three replicates of the assay were averaged and graphed.

Ethics statement. Informed written consent to publish clinical information and photographs of the affected individuals was obtained from the families prior to their involvment in this study, in accordance with IRB-approved protocol 0306-10-HMO (Hadassah Medical Center, Jerusalem, Israel). Further approval for this research was obtained from the West Midlands – Coventry and Warwickshire Research Ethics Committee, Coventry, UK (REC: 20/WM/0098).

Author contributions

TH, VMP, AAL and BAL identified RECQL1 mutant patients, provided clinical information and photographs of the affected individuals. TH and VM analysed whole exome sequencing data. KDB performed segregation analysis and generated patient LCLs. SSJ, SLC and AD performed DNA fibre analysis. LG, JJR, and RH carried out flow cytometry, SCE and chromosome breakage analysis. BLW carried out growth and cytotoxicity assays on LCLs. GSM performed chromatin fraction and immunofluorescence. SJS performed structural modelling. CNM and GLM generated the RECQL1 CRISPR knockout HeLa cell line. GSS generated complemented cell lines, carried out immunofluorescence and co-immunoprecipitation studies and performed Western blotting. SD and JAS purified recombinant RECQL1 and carried out in vitro protein biochemical assays. SD and AD performed cell-based DNA damage sensitivity assays and the COMET assay. ANG generated RECQL1 expression vectors. GMCL and VR carried out C-Fusion 3D high-throughput imaging. GSS, SSJ and RMB planned and supervised the study and wrote the manuscript.

Acknowledgments

We would like to thank the parents and patients from the two RECON Syndrome families for taking part in this study and generously donating tissue samples. We would also like to thank Fay Stewart for help with statistical analysis. GSS, RH, GSM, SLC, AG are funded by a CR-UK Programme Grant (C17183/A23303). SSJ is supported by a project grant funded by the Great Ormond Street Hospital Charity and Sparks (V5019). LJG is supported by a joint funded University of Birmingham and CR-UK Ph.D studentship (C17422/A25154). BLW is supported by a CR-UK Clinical Academic Training Programme award (C11497/A31309). VR lab is supported by funding from the Deutsche Forschungsgemeinschaft (DFG, German Research Foundation)-Project-ID 393547839-SFB 1361, Project-ID 402733153-SPP 2202 and the DFG Major Research Instrumentation Programme (INST 247/845-1 FUGG). JJR is supported by the University of Birmingham. SD, JAS, AD and RMB Jr. were supported in part by the NIH Intramural Research Program, National Institute on Aging (1Z1AAG000741-19). A collaboration to study the identified *RECQL* variant was established via GeneMatcher (48).

References

1. Chu WK, Hickson ID. RecQ helicases: multifunctional genome caretakers. *Nat Rev Cancer.* 2009;9(9):644-654.

2. Croteau DL, et al. Human RecQ helicases in DNA repair, recombination and replication. *Annu Rev Biochem.* 2014;83:519-552.

3. Oshima J, et al. Werner Syndrome: Clinical features, pathogenesis and potential therapeutic interventions. *Ageing Res Rev.* 2017;33:105-114.

4. Cunniff C, et al. Bloom's Syndrome: Clinical spectrum, molecular pathogenesis and cancer predisposition. *Mol Syndromol.* 2017;8(1)4-23.

5. Chan KL, Hickson ID. New insights into the formation and resolution of ultra-fine anaphase bridges. *Semin Cell Dev Biol.* 2011;22(8):906-912.

6. Dongliang M, et al. Human RecQL4 helicase plays multifaceted roles in the genomic stability of normal and cancer cells. *Cancer Lett.* 2018;413:1-10.

7. Sangrithi MN, et al. Initiation of DNA replication requires the RECQL4 protein mutated in Rothmund-Thomson Syndrome. *Cell*. 2005;121:887-898.

8. Lu H, et al. RECQL4 promotes DNA end resection in repair of DNA double strand breaks. *Cell Reports.* 2016;16(1):161-173.

9. Schurman SH, et al. Direct and indirect roles of RECQL4 in modulating base excision repair capacity. *Hum Mol Genet.* 2009;18(18):3470-3483.

10. Seki M, et al. Molecular cloning of cDNA encoding human DNA helicase Q1 which has homology to Escherichia coli Rec Q helicase and localization of the gene at chromosome 12p12. *Nucleic Acids Res.* 1994;22(22):4566-73.

11. Popuri V, et al. The Human RecQ helicases, BLM and RECQ1, display distinct DNA substrate specificities. *J Biol Chem.* 2008;283(26):17766-76.

12. Liu NN, et al. Endogenous Bos Taurus RECQL is predominantly monomeric and more active than oligomers. *Cell Reports.* 2021;36:109688.

13. Sharma S, et al. RECQL, a member of the RecQ family of DNA helicases suppresses chromosomal instability. *Mol Cell Biol.* 2007;27(5):1784-1794.

14. Berti M, et al. Human RECQ1 promotes restart of replication forks reversed by DNA topoisomerase I inhibition. *Nat Struct Mol Biol.* 2013;20(3):347-354.

15. Cybulski C, et al. Germline *RECQL* mutations are associated with breast cancer susceptibility. *Nat Genet.* 2015;47(6):643-646.

16. Sun J, et al. Mutations in RECQL gene are associated with predisposition to breast cancer. *PLoS Genet.* 2015;11(5):e1005228.

17. Sami F, et al. Site-directed mutants of human RECQ1 reveal functional importance of the zinc binding domain. *Mutat Res.* 2016;790:8-18.

18. Cui S, et al. Analysis of the unwinding activity of the dimeric RECQ1 helicase in the presence of human replication protein A. *Nucleic Acids Res.* 2004;32:2158-2170.

19. Sharma S, et al. Biochemical analysis of the DNA unwinding and strand annealing activities catalyzed by human RECQ1. *J Biol Chem.* 2005;280:28072-28084.

20. Banerjee T, et al. Catalytic strand separation by RECQ1 is required for RPA-mediated response to replication stress. *Curr Biol.* 2015;25:2830-2838.

21. Muzzolini L, et al. Different quaternary structures of human RECQ1 are associated with its dual enzymatic activity. *PLoS Biol.* 2007;5:e20.

22. Stewart GS, et al. The DNA double-strand break repair gene *hMRE11* is mutated in individuals with an ataxia-telangiectasia-like disorder. *Cell.* 1999;99(6):577-587.

23. Sharma S, Brosh RM, Jr. Human RECQ1 is a DNA damage responsive protein required for genotoxic stress resistance and suppression of sister chromatid exchanges. *PLoS One*. 2007;110(7):2390-2398.

24. Canela A, et al. Topoisomerase II-induced chromosome breakage and translocation is determined by chromosome architecture and transcriptional activity. *Mol Cell.* 2019;75(2):252-266.

25. Gothe HJ, et al. Spatial Chromosome Folding and Active Transcription Drive DNA Fragility and Formation of Oncogenic MLL Translocations. *Mol Cell.* 2019;75(2):267-283.

26. Thangavel S, et al. DNA2 drives processing and restart of reversed replication forks in human cells. *J Cell Biol.* 2015;208(5):545-62.

27. Zellweger R, et al. Rad51-mediated replication fork reversal is a global response to genotoxic treatments in human cells. *J Cell Biol.* 2015;208(5):563-79.

28. Davies SL, et al. Role for BLM in replication-fork restart and suppression of origin firing after replicative stress. *Nat Struct Mol Biol.* 2007;14(7):677-679.

29. Benedict B, et al. The RECQL helicase prevents replication fork collapse during replication stress. *Life Sci Alliance*. 2020;3(10):e202000668.

30. Wang W, et al. Functional relation among RecQ family helicases RecQL1, RecQL5, and BLM in cell growth and sister chromatid exchange formation. *Mol Cell Biol.* 2003;23(10):3527-35.

31. Nimonkar AV, et al. BLM-DNA2-RPA-MRN and EXO1-BLM-RPA-MRN constitute two DNA end resection machineries for human DNA break repair. *Genes Dev.* 2011;25:350-362.

32. Sangrithi MN, et al. Initiation of DNA replication requires the RECQL4 protein mutated in Rothmund-Thomson Syndrome. *Cell*. 2005;121(6):887-898.

33. Parvathaneni S, et al. Human RECQ1 interacts with Ku70/80 and modulates DNA end-joining of double-strand breaks. *PLoS One.* 2013;8(5):e62481

34. Schnabel F, et al. Premature aging disorders: A clinical and genetic compendium. *Clin Genet.* 2021;99(1):3-28

35. Foo MXR, et al. Premature aging syndromes: From patients to mechanism. *J Dermatol Sci.* 2019;96(2):58-65

36. Bogdanova N, et al. Analysis of a *RECQL* splicing mutation, c.1667_1667+3delAGTA, in breast cancer patients and controls from central Europe. *Fam Cancer.* 2017;16(2):181-186.

37. Li N, et al. Mutations in RECQL are not associated with breast cancer risk in an Australian population. *Nat. Genet.* 2018;50(10):1346-1348.

38. Bahr, et al. Point mutations causing Bloom's syndrome abolish ATPase and DNA helicase activities of the BLM protein. *Oncogene* 1998;17(20):2565-2571.

39. Neff, et al. The DNA helicase activity of BLM is necessary for the correction of the genomic instability of Bloom syndrome cells. *Mol Biol Cell.* 1999;10(3):665-676.521

40. Pike ACW, et al. Structure of the human RECQ1 helicase reveals a putative strand-separation pin. *Proc Natl Acad Sci USA.* 2009;106:1039-1044.

41. Wu L, et al. The HRDC domain of BLM is required for the dissolution of double Holliday junctions. *EMBO J.* 2005;24(14):2679-2687.

42. Boerkoel CF, et al. Mutant chromatin remodeling protein SMARCAL1 causes Schimke immuno-osseous dysplasia. *Nat Genet.* 2002;30:215-220.

43. Poole LA, Cortez D. SMARCAL1 and telomeres: Replicating the troublesome ends. *Nucleus.* 2016;7(3):270-4.

44. Tye S, et al. A fork in the road: Where homologous recombination and stalled replication fork protection part ways. *Semin Cell Dev Biol.* 2020;S1084-9521(19)30093-X.

45. Iannascoli C, et al. The WRN exonuclease domain protects nascent strands from pathological MRE11/EXO1-dependent degradation. *Nucleic Acids Res.* 2015;43(20):9788-9803.

46. Higgs MR, et al. BOD1L is required to suppress deleterious resection of stressed replication forks. *Mol Cell*. 2015;59(3):462-477.

47. Gyori BM, et al. OpenComet: an automated tool for comet assay image analysis. *Redox Biol.* 2014;2:457-65.

48. Sobreira N, et al. GeneMatcher: A matching tool for connecting investigators with an interest in the same gene. *Hum. Mutat.* 2015;36:928–930.

49. Pike ACW, et al. Human RECQ1 helicase-driven DNA unwinding, annealing, and branch migration: Insights from DNA complex structures. *Proc Natl Acad Sci USA.* 2015;112:4286-4291.

Fig. 1

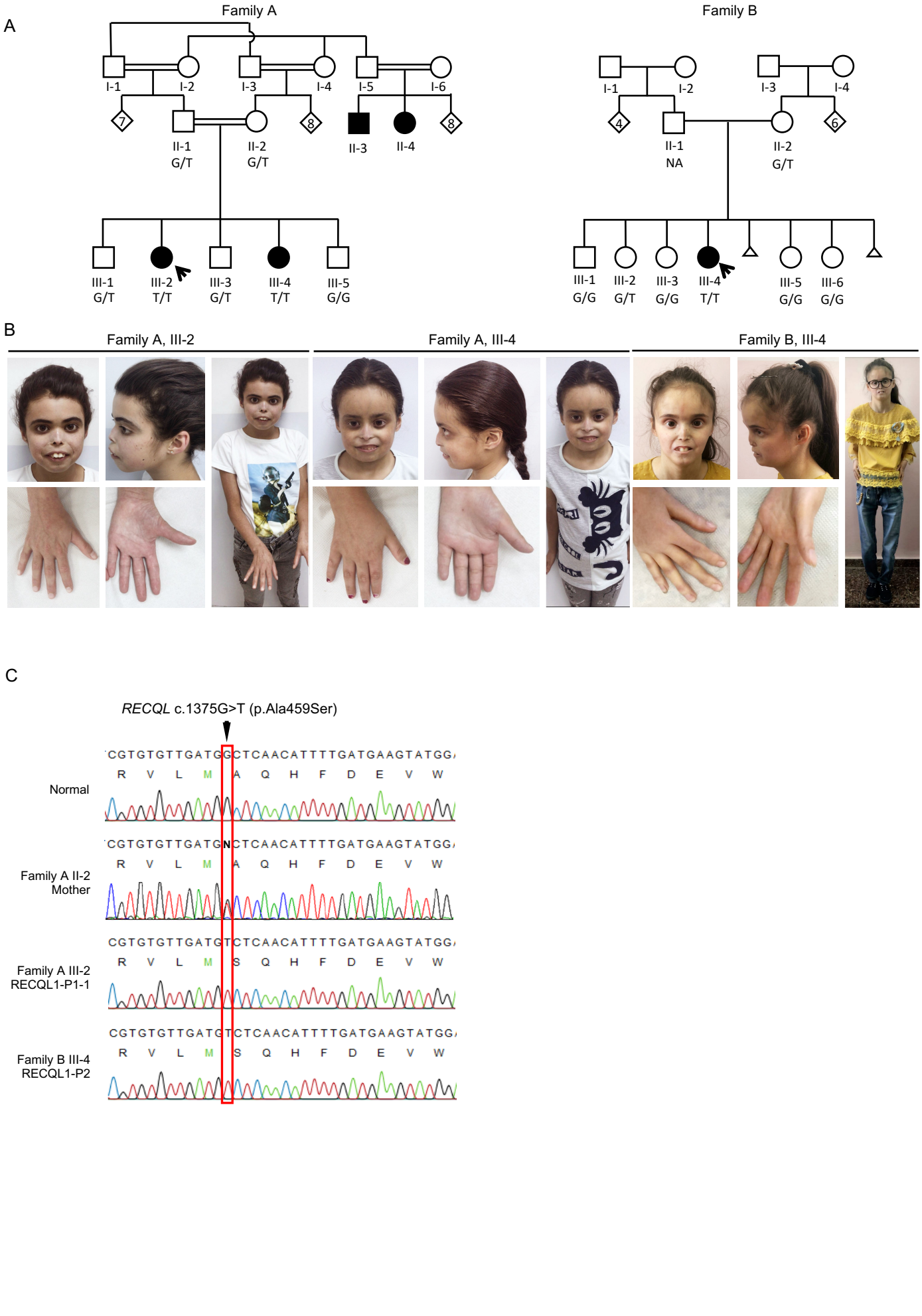
A
Family A
I-1
I-2
I-3
I-4
I-5
I-6
7
8
8
II-1
G/T
II-2
G/T
II-3
II-4
III-1
G/T
III-2
T/T
III-3
G/T
III-4
T/T
III-5
G/G
Family B
I-1
I-2
I-3
I-4
4
6
II-1
NA
II-2
G/T
III-1
G/G
III-2
G/T
III-3
G/G
III-4
T/T
III-5
G/G
III-6
G/G
B
Family A, III-2
Family A, III-4
Family B, III-4
C
RECQL c.1375G>T (p.Ala459Ser)
CGTGTGTTGATGGCTCAACATTTTGATGAAGTATGG
R V L M A Q H F D E V W
Normal
CGTGTGTTGATGNCTCAACATTTTGATGAAGTATGG
R V L M A Q H F D E V W
Family A II-2
Mother
CGTGTGTTGATGTCTCAACATTTTGATGAAGTATGG
R V L M S Q H F D E V W
Family A III-2
RECQL1-P1-1
CGTGTGTTGATGTCTCAACATTTTGATGAAGTATGG
R V L M S Q H F D E V W
Family B III-4
RECQL1-P2

Figure legends

Figure 1. Genealogy of patients with biallelic mutations in *RECQL*. (**A**) Family pedigree of the two families with identified mutations in *RECQL.* Patients III-2 and III-4 from Family A and patient III-4 from Family B are homozygous for the *RECQL* c.1375G>T (NM_032941.2) mutation. Parents and unaffected siblings from both families were either heterozygous or wild type. Where samples were available, genotypes are shown G/G: wild type; G/T: heterozygote; T/T: homozygote. II-3 and II-4 from Family A were reported to have exhibited a clinical phenotype similar to III-2 and III-4. The black arrow indicates affected patients from which cell lines were generated; III-2 from Family A (RECQL1-P1-1) and III-4 from Family B (RECQL1-P2). The small triangle indicates a pregnancy not carried to term. (**B**) Photographs of the affected patients from both families showing distinctive facial characteristics and slender, elongated thumbs. (**C**) Sequencing chromatograms showing the presence of the homozygous c.1375G>T *RECQL* mutation in cDNA derived from the affected patients III-2 (family A) and III-4 (family B) and that the mother from family A (II-2) is heterozygous for the c.1375G>T *RECQL* mutation. Wild type *RECQL* sequence across the position of the mutation is shown.

Fig. 2

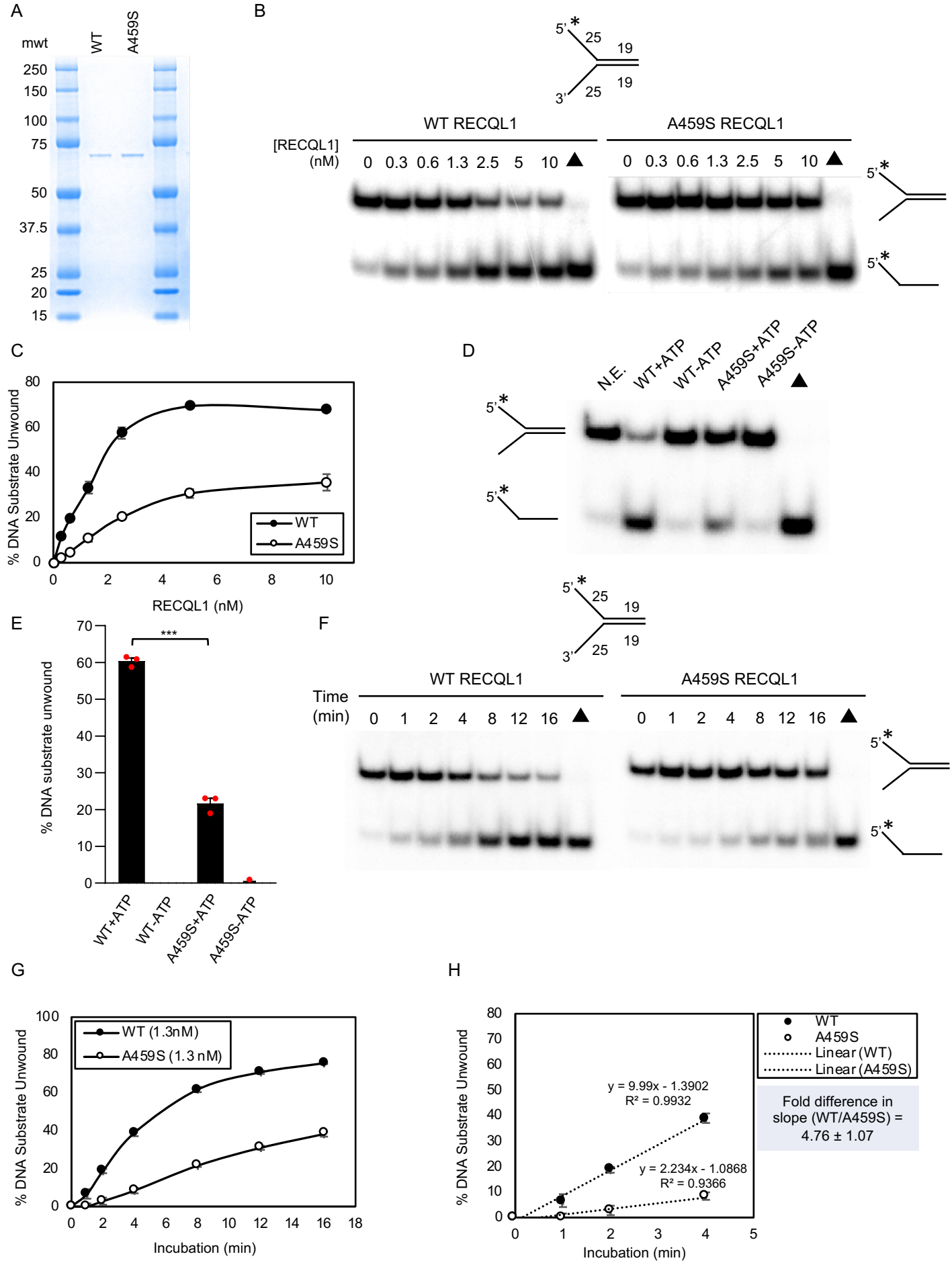
A
mwt
WT
A459S
250
150
100
75
50
37.5
25
20
15
B
5'
25
19
19
3'
25
WT RECQL1
A459S RECQL1
[RECQL1] (nM)
0 0.3 0.6 1.3 2.5 5 10
0 0.3 0.6 1.3 2.5 5 10
5'
5'
C
% DNA Substrate Unwound
RECQL1 (nM)
WT
A459S
D
N.E.
WT+ATP
WT-ATP
A459S+ATP
A459S-ATP
5'
5'
E
% DNA substrate unwound
***
WT+ATP
WT-ATP
A459S+ATP
A459S-ATP
F
5'
25
19
3'
25
19
WT RECQL1
A459S RECQL1
Time (min)
0 1 2 4 8 12 16
0 1 2 4 8 12 16
5'
5'
G
% DNA Substrate Unwound
WT (1.3nM)
A459S (1.3 nM)
Incubation (min)
H
% DNA Substrate Unwound
y = 9.99x - 1.3902
R² = 0.9932
y = 2.234x - 1.0868
R² = 0.9366
WT
A459S
Linear (WT)
Linear (A459S)
Fold difference in slope (WT/A459S) = 4.76 ± 1.07
Incubation (min)

Figure 2. The p.A459S mutation compromises RECQL1 helicase activity. (**A**) SDS polyacrylamide gel stained with Coomassie showing recombinant human RECQL1-WT and RECQL1-A459S (500 ng each). (**B**) Specified RECQL1 concentrations were tested for unwinding a radiolabelled 19-bp forked duplex DNA substrate (0.5 nM) in 15 min. Representative gels are shown. Star indicates a 5´ radiolabel on the 19 bp forked duplex DNA substrate. Black triangle indicates heat-denatured DNA substrate control used as a marker for duplex unwinding. (**C**) Quantitation of DNA unwinding from three independent experiments with SEM. Area under the curve (AUC): WT (mean±SEM: 578.3±8.01); A459S (mean±SEM: 254.3±18.63). WT vs A459S AUC unpaired t-test: $p<0.0001$. (**D**) Representative gels showing analysis of helicase activity catalyzed by RECQL1 (2.5 nM) on a 19 bp forked DNA substrate in the presence or absence of 5 mM ATP as indicated. (**E**) Quantitation of DNA unwinding from three independent experiments with SEM. (**F**) Kinetic analyses of unwinding by RECQL1-WT or RECQL1-A459S. Representative gel images showing analysis of reaction mixtures containing 1.3 nM RECQL1-WT or RECQL1-A459S helicase incubated with a 19 bp forked duplex DNA substrate for the indicated times. (**G**) Quantitation of DNA unwinding from three independent experiments with SEM. (**H**) Quantitation of DNA unwinding showing a linear trendline and slope of unwinding from three independent experiments with SEM. AUC: WT (mean±SEM: 830.3±11.35); A459S (mean±SEM: 316.1±10.3). WT vs A459S AUC unpaired t-test: $p<0.0001$. (* $p<0.05$; ** $p<0.01$; *** $p<0.001$)

Fig. 3

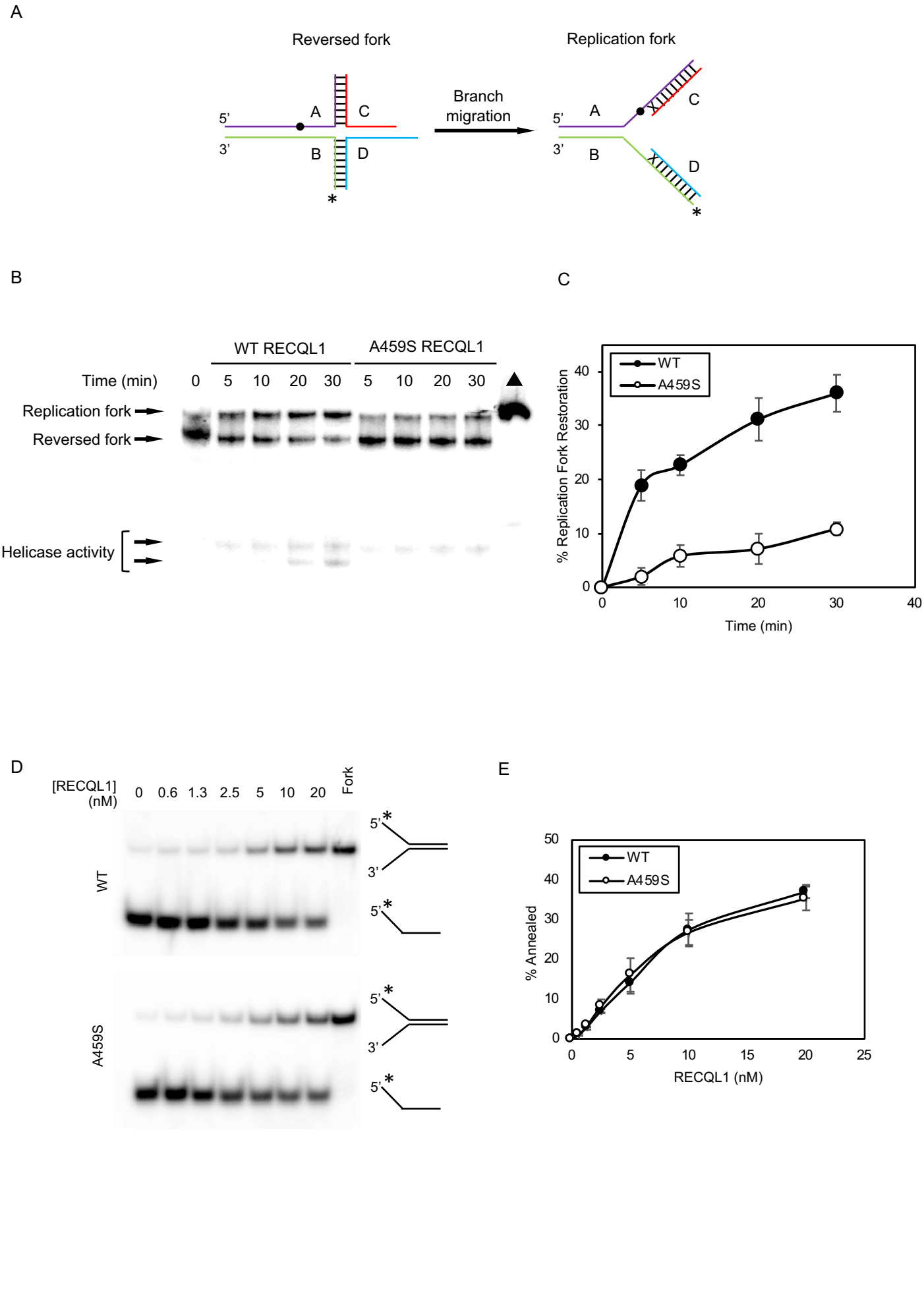
A
Reversed fork
Replication fork
Branch migration
5'
3'
A
B
C
D
*
X
B
WT RECQL1
A459S RECQL1
Time (min)
0 5 10 20 30 5 10 20 30
Replication fork
Reversed fork
Helicase activity
C
% Replication Fork Restoration
WT
A459S
Time (min)
D
[RECQL1] (nM)
0 0.6 1.3 2.5 5 10 20 Fork
WT
A459S
E
% Annealed
WT
A459S
RECQL1 (nM)

Figure 3. The p.A459S mutation compromises the ability of RECQL1 to remodel reversed replication forks but not catalyse single strand annealing. (**A**) Depiction of the reversed and replication fork substrates used in this experiment. The black dot and 'X' in the figure represent an isocytosine base and mismatched bases respectively. These were added to minimize spontaneous conversion of the reversed fork into replication fork. The star indicates the 5' end of the oligo that was radiolabelled with ^{32}P. (**B**) WT and A459S RECQL1 (20 nM) was incubated with 2 nM radiolabelled reversed fork substrate at 37 °C for the times indicated. 2 nM radiolabelled replication fork (black triangle) was included as a marker. A representative gel is shown. (**C**) Quantitation of DNA unwinding from three independent experiments with SEM. Area under the curve (AUC): WT (mean±SEM: 709.5±35.23); A459S (mean±SEM: 174.4±23.91). WT vs A459S AUC unpaired t-test: $p<0.0002$. **(D** and **E)** RECQL1 strand annealing activity was assessed by the formation of a 19 bp forked duplex DNA molecule from two partially complementary single-stranded oligonucleotides as a function of increasing RECQL1 concentration. (**D**) Two partially complementary oligonucleotides (one radiolabelled at the 5′-end and the other unlabelled; 0.5 nM each were incubated with the indicated concentrations of RECQL1 for 15 min at 37 °C in the absence of ATP. A 19 bp forked duplex was loaded as a marker. Representative gel images are shown. (**E**) Quantitation of strand annealing activity from three independent experiments with SEM.

Fig. 4

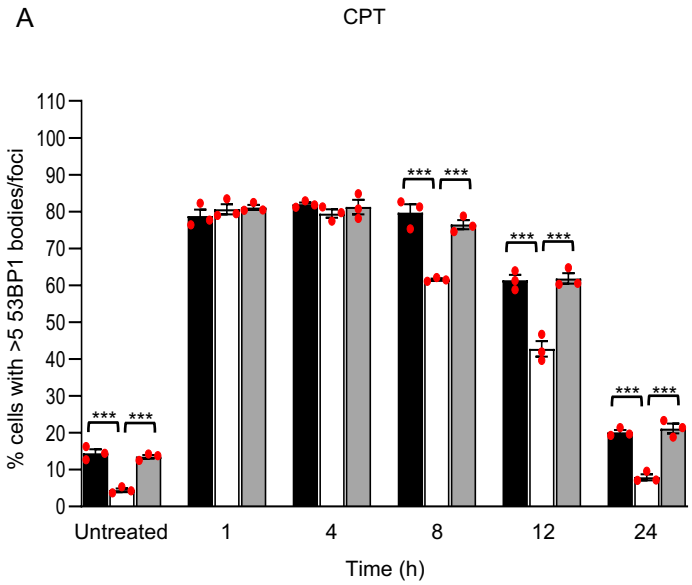
A
CPT
% cells with >5 53BP1 bodies/foci
Untreated
1
4
8
12
24
Time (h)

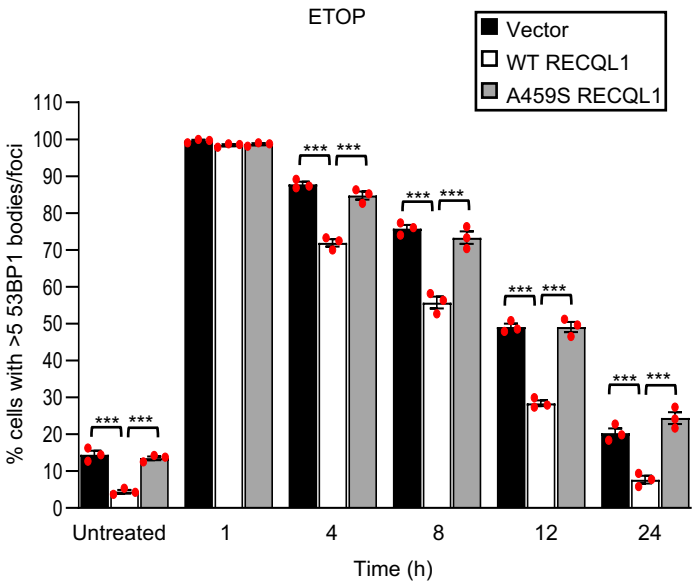
ETOP
Vector
WT RECQL1
A459S RECQL1
% cells with >5 53BP1 bodies/foci
Untreated
1
4
8
12
24
Time (h)

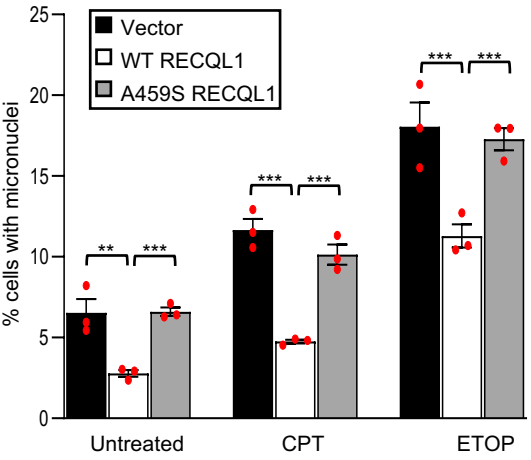
B
Vector
WT RECQL1
A459S RECQL1
% cells with micronuclei
Untreated
CPT
ETOP

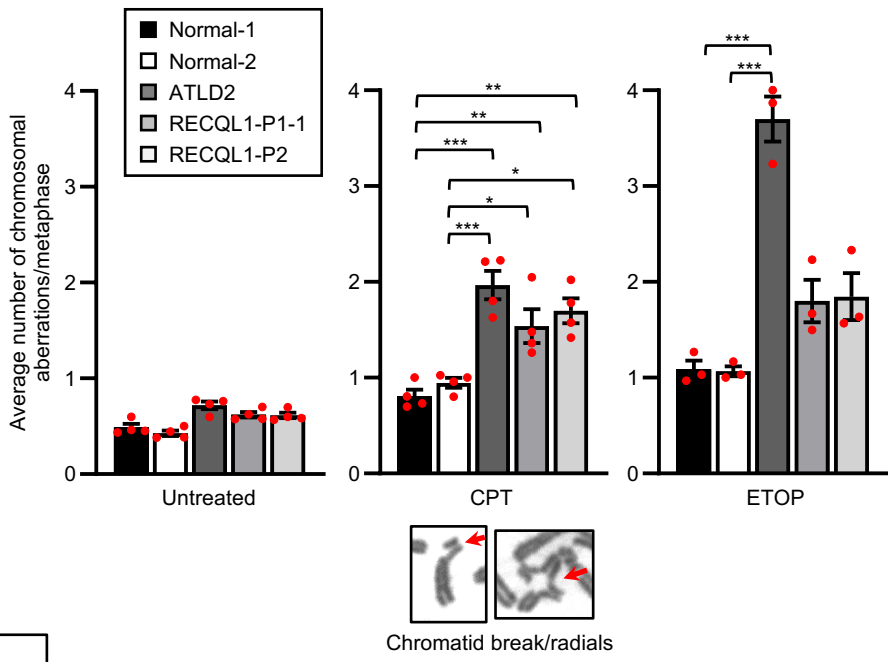
C
Normal-1
Normal-2
ATLD2
RECQL1-P1-1
RECQL1-P2
Average number of chromosomal aberrations/metaphase
Untreated
CPT
ETOP
Chromatid break/radials

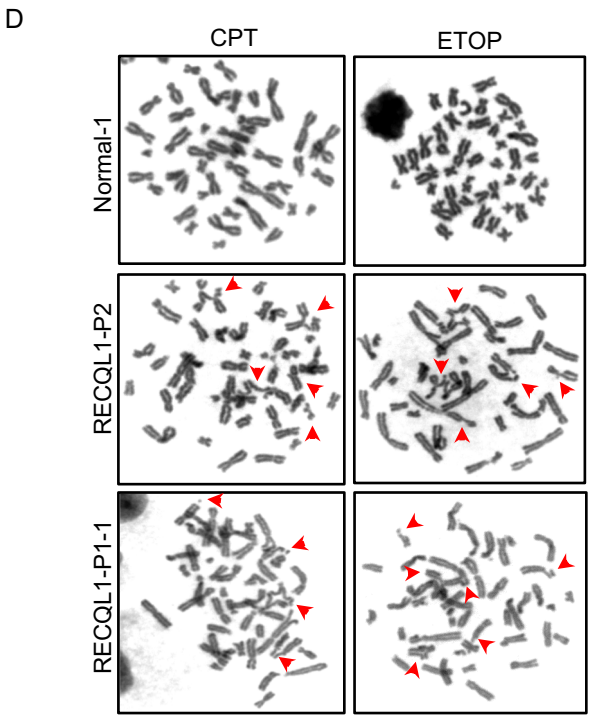
D
CPT
ETOP
Normal-1
RECQL1-P2
RECQL1-P1-1

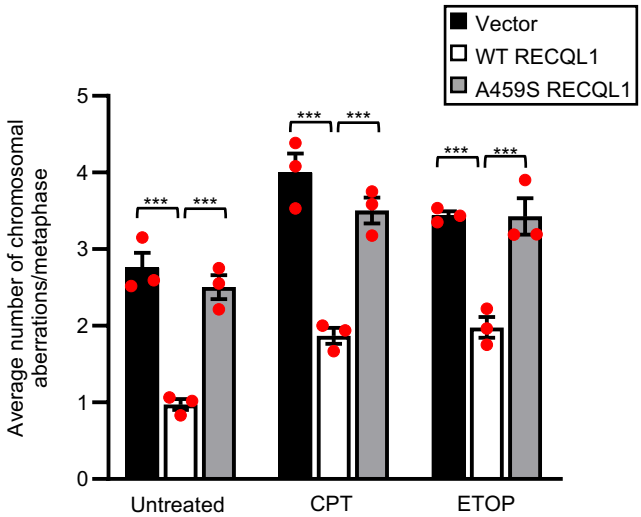
Vector
WT RECQL1
A459S RECQL1
Average number of chromosomal aberrations/metaphase
Untreated
CPT
ETOP

Figure 4. Complementation of RECQL1-P1-1 fibroblasts with WT RECQL1 restores normal repair of DNA damaged induced by CPT and ETOP. (**A**) Quantification of 53BP1 foci in complemented patient RECQL1-P1-1 fibroblasts before and after treatment with 100 nM CPT (1 h) and 1 μM ETOP (30 min). 53BP1 foci in untreated cells and cells 24 h post-DNA damage induction were quantified in G1 phase only (mitosin negative) to assess the amount of replication damage induced by CPT/ETOP that has transited into the following cell cycle. 53BP1 foci in cells 1-12 h post-DNA damage induction were quantified in S/G2 phase only (mitosin positive) to monitor the kinetics of repair in damaged S/G2-phase cells. The mean of three independent experiments is shown with the SEM. A minimum of 300 cells were counted per time point. Statistical significance was calculated using a two-way ANOVA with Tukey's multiple comparison. (**B**) Micronuclei were quantified from cells described in (A) before and 24 h after exposure to CPT and ETOP. The mean of three independent experiments is shown with the SEM. A minimum of 500 cells were counted per time point. Statistical significance was calculated using a two-way ANOVA with Tukey's multiple comparison. (**C** and **D**) Quantification of chromosome aberrations in (C) two normal LCLs, two RECQL mutant LCLs and an ATLD LCL and (D) complemented patient RECQL1-P1-1 fibroblasts before and 24 h after chronic exposure to low dose CPT (5 nM) and ETOP (50 nM). Chromosome aberrations includes chromatid/chromosome gaps/breaks, chromatid/chromosome fragments and chromosome radials/exchanges. Representative images of each type of aberration are shown. The mean of three independent experiments is shown with the SEM. A minimum of 50 metaphases were counted per cell line in each experiment. Statistical significance was calculated using a two-way ANOVA with Tukey's multiple comparison. (* $p<0.05$; ** $p<0.01$; *** $p<0.001$).

Fig. 5

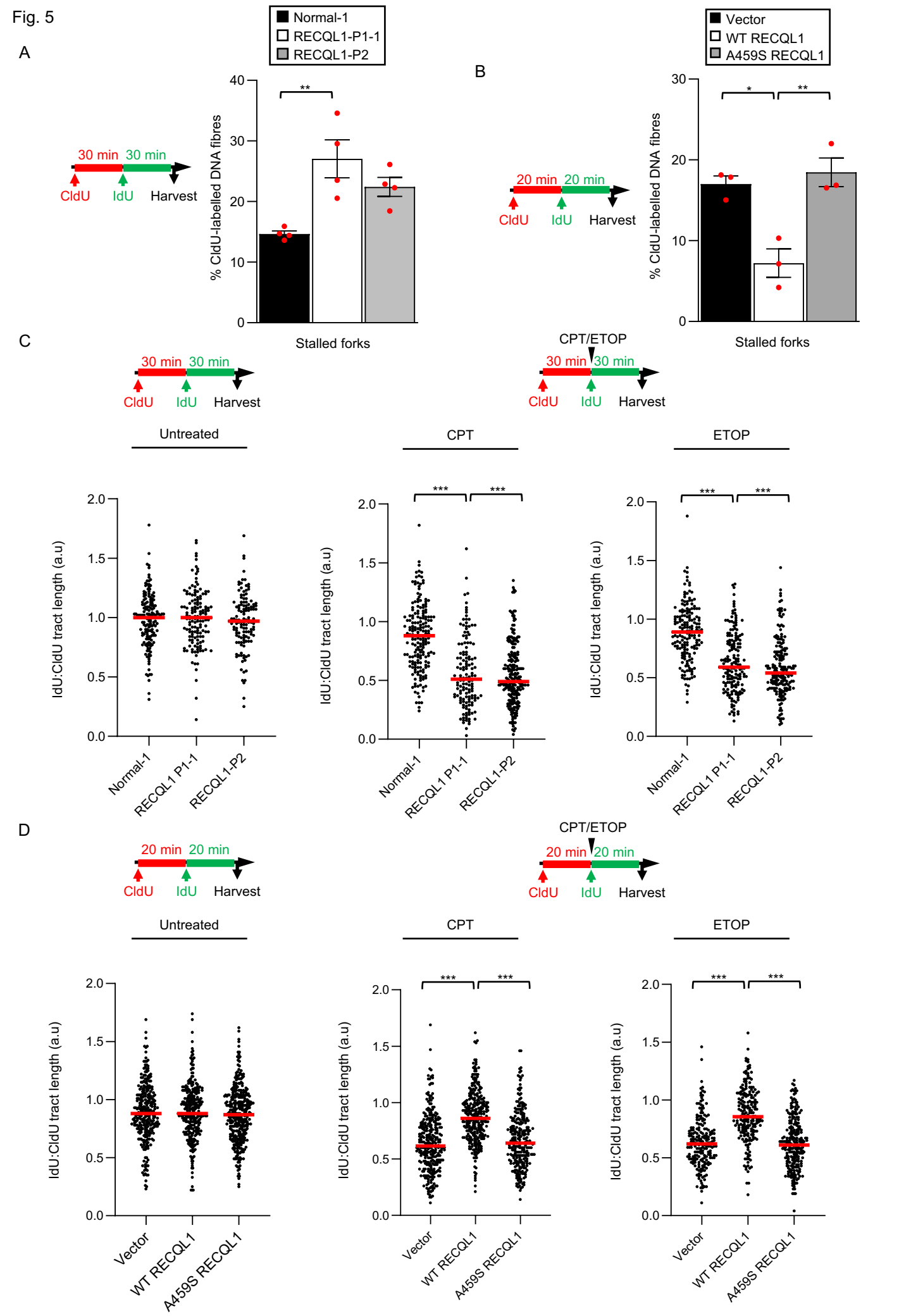
A
Normal-1
RECQL1-P1-1
RECQL1-P2
30 min 30 min
CldU
IdU
Harvest
% CldU-labelled DNA fibres
Stalled forks
B
Vector
WT RECQL1
A459S RECQL1
20 min 20 min
C
CPT/ETOP
Untreated
CPT
ETOP
IdU:CldU tract length (a.u)
Normal-1
RECQL1 P1-1
RECQL1-P2
D
Vector
WT RECQL1
A459S RECQL1

Figure 5. RECON patient cells display a reduced efficiency of replication in the presence of TOP1/2 inhibitors. (**A**) LCLs and (**B**) complemented RECQL1-P1-1 patient fibroblasts were sequentially labelled with CldU (red) and IdU (green) as shown. Stalled forks (red only tracks) were quantified. The mean of four independent experiments is shown. A minimum of 200 forks were counted per condition. Statistical significance was calculated using a one-way ANOVA with Tukey's multiple comparison. (**C**) LCLs and (**D**) complemented fibroblasts were sequentially labelled with CldU and IdU (+/- 50nM CPT or ETOP) as shown. The length of the CldU and IdU tracks of dual labelled DNA fibres (>150 per condition) were measured and a ratio of IdU:CldU track length was calculated, which represents the efficiency of replication in the presence/absence of CPT/ETOP. The median of three independent experiments is shown (red line). Statistical significance was calculated using a Kruskal-Wallis test with Dunn's multiple comparison. (*p<0.05; **p<0.001; ***p<0.0001).

Fig. 6

A

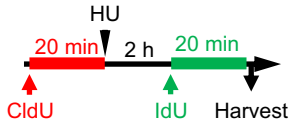
HU
20 min
2 h
20 min
CldU
IdU
Harvest

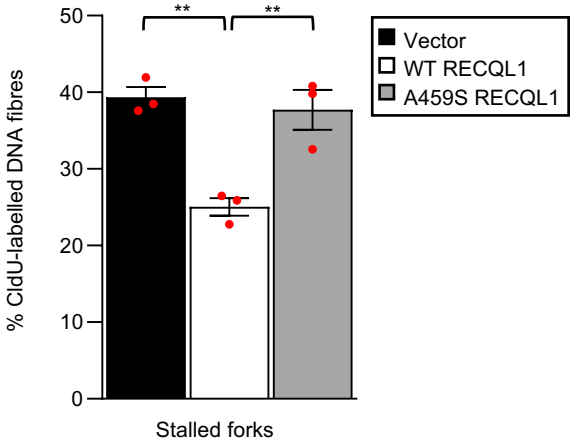
% CldU-labelled DNA fibres
50
40
30
20
10
0
**
**
Vector
WT RECQL1
A459S RECQL1
Stalled forks

B

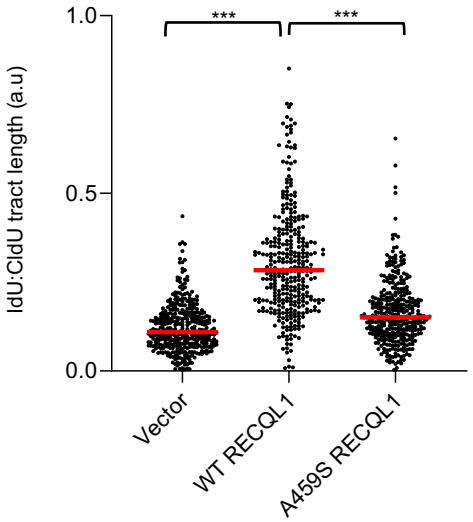
IdU:CldU tract length (a.u)
1.0
0.5
0.0
***
***
Vector
WT RECQL1
A459S RECQL1

C

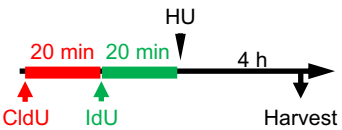
HU
20 min
20 min
4 h
CldU
IdU
Harvest

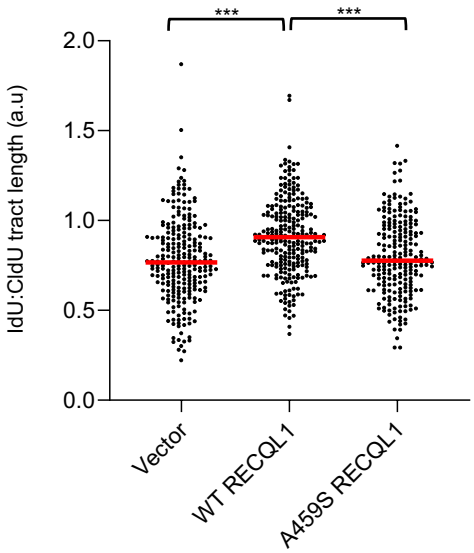
IdU:CldU tract length (a.u)
2.0
1.5
1.0
0.5
0.0
***
***
Vector
WT RECQL1
A459S RECQL1

Figure 6. RECON patient cells exhibit reduced replication fork restart and increased replication fork degradation following exposure to HU. (**A**). Complemented RECQL1-P1-1 patient fibroblasts were labelled with CldU and IdU following exposure to 2 mM HU as shown. Stalled forks were quantified. The mean of three independent experiments is shown. A minimum of 200 forks were counted per condition. Statistical significance was calculated using a one-way ANOVA with Tukey's multiple comparison. (**B**) Cells from (A) were labelled with CldU and IdU as shown in (A). The IdU:CldU ratio was calculated for a minimum of 100 forks per condition from three independent repeats. The IdU:CldU ratio represents the efficiency of replication in the absence HU and efficiency of replication fork restart following removal of HU. (**C**) Cells from (A) were labelled with CldU and IdU then exposed to 4mM HU as shown. The IdU:CldU ratio was calculated for a minimum of 100 forks per condition from three independent experiments. An IdU:CldU ratio <1 indicates replication fork degradation. Statistical significance was calculated using a Kruskal-Wallis test with Dunn's multiple comparison (B-C). (*p<0.05; **p<0.001; ***p<0.0001).

Fig. 7

A

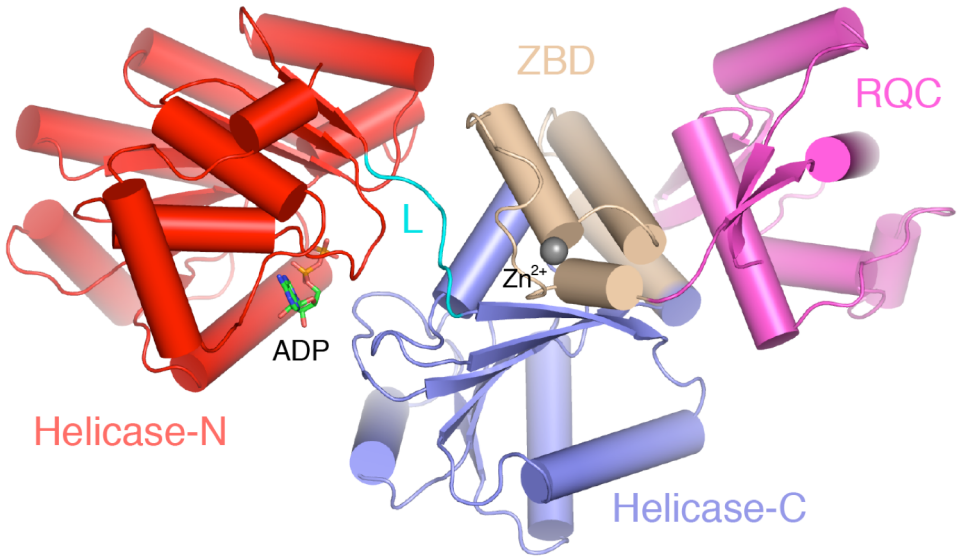
ZBD
RQC
L
Zn2+
ADP
Helicase-N
Helicase-C

B

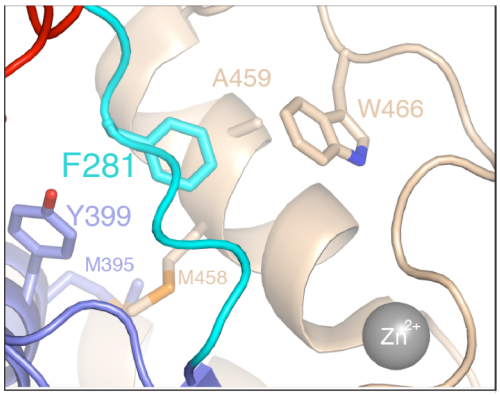
A459
W466
F281
Y399
M395
M458
Zn2+

C

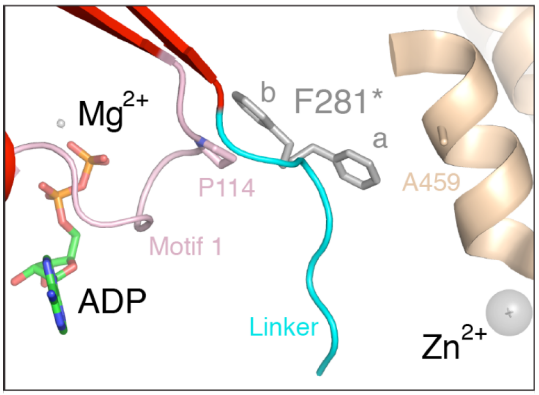
Mg2+
b
F281*
a
P114
A459
Motif 1
ADP
Linker
Zn2+

Figure 7. Structural modelling of the RECQL1 p.A459S mutation. (**A**) Overall structure of the RECQL1 monomer shown in a ribbons representation with the individual domains coloured according to Supplementary Figure 1A. The grey sphere represents the Zn^{2+} ion within the ZBD and the GDP is shown as sticks. (**B**) A459 forms part of an extended hydrophobic cluster involving W466 and M458 from the ZBD, M395 and Y359 from the helicase-C domain and F281 from the helicase linker (cyan). (**C**) Two conformations of F281 within the helicase linker observed in the GDP-bound structure suggest a molecular basis for the dynamic coupling of structural perturbations in the ZBD to ATPase/helicase activity. The P-loop is highlighted in light pink. Conformation 'b' of F281 stacks against the P144 pyrrolidine ring whilst conformation 'a' packs against A459. Figure produced using PyMOL (https://pymol.org/2/) and coordinates from PDB accessions 2V1X and 2WWY (40, 49).

Table 1. Clinical description of the *RECQL* mutant patients.

		Family A		Family B
Patient		III-2 (RECQL1-P1-1)	III-4 (RECQL1-P1-2)	III-4 (RECQL1-P2)
Mutation 1		c.1375G>T; p.Ala459Ser	c.1375G>T; p.Ala459Ser	c.1375G>T; p.Ala459Ser
Mutation 2		c.1375G>T; p.Ala459Ser	c.1375G>T; p.Ala459Ser	c.1375G>T; p.Ala459Ser
Cell line		RECQL1-P1-1	RECQL1-P1-2	RECQL1-P2
Sex		F	F	F
Clinical features				
Gestation (weeks)		Term	Term	Term
Age of last investigation		9y 8m	4y 0m	14y 9m
Head circumference - Birth		N/A	N/A	N/A
Head circumference - Current (Z score)		50 cm (-1.64)	47.8 cm (-1.18)	50.8 cm (-2.92)
Length - Birth		N/A	N/A	N/A
Height - Current (Z score)		123.8 cm (-1.98)	96.4 cm (-1.02)	138.4 cm (-3.59)
Weight - Birth		~3 kg	~3 kg	3.5 kg
Weight - Current (Z score)		22.5 kg (-2.05)	13.9 kg (-1.05)	22.1 kg (-8.47)
Growth retardation		Yes	No	Yes
Learning difficulties		No	No	No
Skin abnormalities		Photosensitivity; livedo reticularis; keratosis pilaris; xeroderma	Photosensitivity; xeroderma	Photosensitivity; thin skin; scaling; hirsutism; xeroderma
Facial abnormalities		Round face, redness of eyes, tiny, pinched nose with anteverted nares, prominent premaxilla, smooth philtrum, progeroid appearance	Red eyes, tiny, pinched nose with anteverted nares, prominent premaxilla, smooth philtrum, progeroid appearance	mask senile-like face (progeroid), deep set eyes, absent lower lid eyelashes, small ears with small, attached earlobes, prominent nasal bridge with a tiny, pinched nose with hypoplastic ala nasi, prominent premaxilla, thin lips and smooth philtrum.
Eye abnormalities		Xerophthalmia, eyes remain open during sleep	Xerophthalmia	Deep set eyes, hypoplastic/absent eye lashes
Skeletal abnormalities		Slender, elongated thumbs with hyperconvex nails; slight hyperextension of elbows	Slender, elongated thumbs with proximal insertion; hirsutism of back, minor joint laxity	Slender, elongated thumbs with hyperconvex nails, arachnodactyly; slight hyperextension of elbows; severe wasting of muscles
Other abnormalities		Delayed eruption of permanent teeth		Irregular, crowded teeth with delayed eruption of permanent teeth
Immunology	Recurrent infections	No	No	Early childhood; resolved
	Anaemia	No	No	Yes
	Neutropenia	No	No	No
	Immunoglobulins	N/A	N/A	N/A
	Other			Thrombocytopenia

Table 2. Comparison of the k_{cat} (s^{-1}), K_m (μM) and V_{max} (nM/s) for ATP hydrolysis by RECQL1-WT and RECQL1-A459S.

Protein	k_{cat} (s^{-1})[a]	K_m (μM)[b]	V_{max} (nM/s)
RECQL1-WT	103.5 ± 7.7	95.3 ± 8.2	28.3 ± 5.7
RECQL1-A459S	37.3 ± 13.3	48.4 ± 16.4	8.4 ± 2.8

[a] Reaction mixtures contained M13mp18 ssDNA (32 mM nucleotide phosphate), 1 mM ATP, and 20 nM RECQL1.
[b] Reaction mixtures contained M13mp18 (32 mM nucleotide phosphate), 31.3 μM – 2 mM ATP range, and 40 nM RECQL1.